An Alternative Approach to Free Space Optical Communication Link

By

Okan KARATAY

**A Dissertation Submitted to the
Graduate School in Partial Fulfillment of the
Requirements for the Degree of**

MASTER OF SCIENCE

**Department: Electrical and Electronics Engineering
Major: Electronics and Communication**

**İzmir Institute of Technology
İzmir, Turkey**

July, 2004

ACKNOWLEDGEMENT

I am very grateful to my supervisor Asst. Prof. Dr. M. Salih Dinleyici for his support and guidance throughout my research. His comments and advices directed me to do best.

I also offer my special thanks to Asst. Prof. Dr. Mustafa A. Altınkaya for his advices and comments during the thesis study.

And finally, I wish to express my gratitude to my family, the source of my motivation. To finish this thesis in success would be harder without their continued support and encouragement.

ABSTRACT

In recent years commercial and military interest in free-space optical (FSO) communication has been growing due to advantages of high bandwidths, portability and high security. Despite of the numerous advantages, atmospheric events such as attenuation and scintillation severely affects the link quality. Novel methods of mitigating atmospheric events have been applied. Usage of large aperture lenses and high transmitted power decreases the degradation effects, but increases the overall system cost. Fresnel lenses, as an alternative to the classical optic system for mitigating scintillation effects would be a low-cost solution. As a result of the technological improvements on output power and divergence angles of VCSEL (Vertical Cavity Surface Emitting Laser) high-speed cost effective FSO communication system design became possible. In this thesis commercially available FSO systems are reviewed and an alternative low-cost system relying on Fresnel lens optical unit is theoretically and experimentally investigated. The system has been tested and compared for two-day periods with various configurations under atmospheric effects. The results indicated that the Fresnel lenses perform comparably well in contrast to bulk optic lenses. Thus, the large aperture Fresnel optic unit can be deployed for better performance at the scintillation dominating situation without a penalty at the cost.

ÖZ

Serbest-uzay optik iletişim son yıllarda gerek askeri gerekse de sivil iletişim alanlarında yüksek iletişim kapasitesi, çabuk kurulumu, taşınabilinirliği ve dar bir saçılma açısına bağlı güvenlik özellikleri ile dikkat çekmektedir. Ancak, iletim kanalının atmosfer olması link kalitesi üzerinde ışıldama ve yüksek zayıflamadan kaynaklanan olumsuz etkilere neden olmaktadır. Bu zorlukları aşmak için bir çok farklı donanım ve iletişim tekniği kullanılmaktadır. Düşük güçlerde iletişime olanak sağlayan ve ışıldamanın azaltılmasına da yarayan büyük çaplı merçeklerin kullanımı sistem maliyetini oldukça olumsuz etkilemektedir. Klasik optik mercekler yerine Fresnel merceklerinin kullanılması hem ışıldama hem de maliyet için bir çözüm olabilmektedir. VCSEL (Vertical Cavity Surface Emitting Laser) teknolojisindeki gelişmelere bağlı olarak, yüksek çıkış güçlü az saçılan bu lazerler daha düşük maliyetli serbest-uzay iletim hatlarının tasarlanmasını olanaklı kılmaya başlamıştır. Bu tez çalışmasında var olan sistemler incelenmekte ve Fresnel merceklerin kullanıldığı alternatif düşük-maliyetli serbest-uzay optik iletişim sistemi teorik ve deneysel olarak incelenmiştir. İletişim sistemi atmosferik iletim kanalında değişik optik düzenekler ile iki günlük dönemsel süreler boyunca gözlemlenmiştir. Deneysel sonuçlar Fresnel merceklerin klasik merceklere benzer başarımlara ulaştığını göstermektedir. Sonuç olarak büyük çaplı Fresnel mercekli sistemler ışıldamanın baskın olduğu iletim kanalında maliyeti artırmadan daha iyi başarım elde etmede kullanılabilmektedir.

TABLE OF CONTENTS

LIST OF FIGURES

LIST OF TABLES

Chapter 1

INTRODUCTION

From the dawn of civilisation, communication has been one of the principle needs of mankind. This need has created great interest in devising communication systems for sending messages from one distant place to another. Since the ancient times different forms of communication systems have been evolved. The main idea behind all of these techniques is to send information from a place to another without corrupting the interested data. Not even long before the 19th century most of the communication is realised with postal services or some simple line-off-sight optical systems like smoke. The invention of the telegraph by Samuel F. B. Morse in 1838 was a revolutionary advance in communication systems, which was then called as the beginning of the electrical communication era. [1]

Electrical communication systems use electromagnetic spectrum for carrying information where the data is transferred through the communication channel by carrier, which is commonly a sinusoidal signal. At the receiving system the transmitted information is demodulated from the carrier. Information capacity of these systems related to the carrier frequency, which is increased as the frequency increases. As a result higher frequencies (shorter wavelengths) are employed for larger information capacities. Radio, television, radar, and microwave links could be considered under these systems.

In addition to the electrical systems another important communication technique is optical communication, which uses the optical frequency radiation region of electromagnetic spectrum. Different from the electrical communication in the optical communication information is transmitted by modulating the intensity of optical power, which is called intensity modulation (IM). Optical communication systems are classified according to their transmission medium: guided systems such as fiber-communication and unguided systems like free-space optical communication (FSOC), which is the concept, covered in this thesis.

By the end of 19th century interactions between nations in means of trade, policy etc. grows rapidly, which is resulted with an increase in the amount of knowledge transmitted. Early in the 20th century nearly all of the transmitted knowledge was in

acoustical form which needs not more than a few kHz of bandwidth for communication but after the emerge of Internet in 1990s demand on high data rated communication has increased. Internet handles a number of services such as home shopping, video-on-demand, remote education, and videoconferencing. This demand is raised with the PCs, which facilitates the access to the Internet. To handle the exponentially increasing demand for high-bandwidth services new transmission mediums and systems are being researched. Light wave communication, which is one of the alternative communication systems, sufficiently fulfil this demand that uses fiber (guided) and free space (unguided) as transmission medium while supplying several Gbps speeds.

Light-wave communication as stated previously may be classified according to the transmission medium that can be guided medium or unguided-medium. The guided transmission is based on the propagation of the light through a guided media such as fiber, which is outside the scope of this thesis. Unguided propagation is the transmission of light through air or space with the absence of the guiding media. Unguided systems most commonly called as Free Space Optical Communication (FSOC) or Optical Wireless Communication (OWC) systems.

The idea of using light in communication through unguided optical medium goes as far back as the 19^{th} century. Alexander Graham Bell invented the photophone, which was a simple phone that uses light in place of electrical signals. Despite the long historical background unguided optical communication did not take interest of researches because of the technological obstacles. With the advent of technology, optical communication systems through guided or unguided medium attracted great deal of researches between 1960 and 1970 [2]. The years following 1970, guided optical transmission (fiber-optic) dominates the light wave communication with their high bandwidth and long distant transmission capability. More recently with the increasing interest on wireless communication and technological improvements, the interest on unguided optical (FSO) communication is raised again. Although significant advances have been made over past decade, the idea of FSO remains relatively simple: light is transmitted from the transmission station through atmosphere to the receiver station in a form of a small divergent beam. Theoretically FSO communication is possible as long as the link budget overcomes the degrading effects such as atmospheric attenuation, scintillation and coupling losses.

FSO attracts the communication market with their challenging bandwidth capability and plug and play installation. Similar to the fiber-optic communication FSO

systems use near infrared (IR) frequency band of electromagnetic spectrum (750nm-1600nm). Moreover, unlike the other competing wireless technologies in FSO IR band is unlicensed worldwide and does not require spectrum fees. Commercially available FSO systems tend to operate in two different frequency bands in IR spectrum: 780-900nm and 1500-1600nm. Lasers in the 780-900nm band are less expensive (VCSELs hit the market with the available speeds up to 3 Gbps with a cost of $30 versus DFB lasers in same speeds which costs $1000) and therefore are usually preferred for applications over moderate distances. In contrast to fiber optic systems 1300nm-frequency band is not used by FSO manufacturers due to high attenuation in the atmosphere at that frequency window.

Typical FSO systems use ON-OFF keying (OOK) as a modulation format due to its simplicity, which is also widely applied in fiber optic technology. OOK method is based on the transmission of data in form of “1”s and “0”s where light on represents “1” and light off represents “0”. This simple modulation scheme allows FSO systems to be designed free from transmission protocols called as protocol transparent. Available FSO systems offer capacities in the range of 100Mbps to 2.5Gbps [3, 4, 5].

1.1 Applications

FSO systems today are applied in various areas, which are grouped below:

- *Network extensions*: One of the application areas of FSO is the extension of fiber rings to connect new networks rings, see figure 1.1. Deployment of present wireline transmission systems such as fiber or copper lines generally encounters natural obstacles such as streets, rivers that prevent line installation. Furthermore establishing wireless systems in such cases is over costly while considering short distance communication application and licence issues.

- *Last-Mile access*: In today’s cities more than %95 of the buildings do not have access to the fiber optic infrastructure due to the development of communication systems after the metropolitan areas. FSO technology seems a promising solution to the connection of end-users to the service providers or to other

existing networks. Moreover FSO provides high-speed connection up to Gbps, which is far more beyond the alternative systems.

- *Military Systems*: FSO technology has numerous features that attract military interest. The easy and rapid deployment, high-speed transmission rates and security due to the divergent IR light make these systems an interesting alternative for defensive usage.

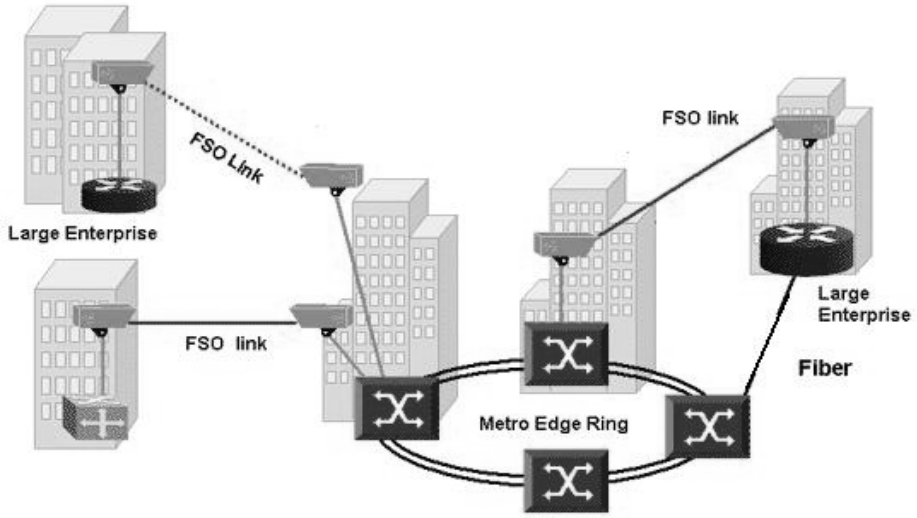

Figure 1.1. Competitive local exchange carrier as a connecting point of optical network ring, which is also connecting to a regional fiber ring. The two buildings at the center side are connected through fiber-optic cables and the three building on the left and right are connected through FSO [6].

In addition to the major application areas, quick deployment, easy transportation and plug-and-play features of FSO communication make these systems applicable in conference and sport event organisations where short-term high-speed communication is needed. Until recently, FSO is applied mostly for network extensions, which is a major problem as stated above.

By the end of 1990s FSO market grew rapidly and attracted many manufacturers to the unguided-wave optics. For example in United States most of the buildings that do not have access to the existing fiber backhaul are within 1.5km of area. Establishing connecting to these buildings with fiber can cost US $100 000- $200 000 per km in metropolitan areas where most of the cost is originated from fiber trenching [6]. As a

result, several companies have begun field trails worldwide for the availability of FSO systems under different conditions. Moreover many service providers hit the market with their high-speed systems at an affordable price, which encourages researches on FSO.

1.2 Advantages and Disadvantages

1.2.1 Advantages

Main advantages of FSO communication systems over other standard wireless and wireline communication system are cost, transmission rate, deployment, licensing, portability and security.

- *Cost:* One of the main advantages of FSO systems is the total cost reduction in contrast to the fiber optic systems. For example, fiber deployment in urban areas could cost $300 000-$700 000 per kilometer without other installation costs like fees and digging. A FSO link with same transmission rates could be affordable at a price of $18.000 [6, 7]. In addition to this FSO links have an information capacity, which decreases the overall transmission cost per bits while comparing with the competing copper-line transmission systems.

- *Transmission rate:* Today old-fashioned copper transmission lines or radio frequency (RF) systems either license free or not, can transmit data much farther than FSO, but these systems are bandwidth limited. Furthermore fiber optic systems as stated above are not cost-effective while calculating cost/km. Commercial FSO systems on market provide bandwidths up to 2.5Gbps. 160Gbps have been tested in laboratories; speeds in theory achievable up to Terabit range [5, 8].

- *Deployment:* In contrast to other wireline systems FSO does not require any permission for digging or other concerns that prevent deploying communication system. Typical FSO links are installed on rooftop of buildings or office windows that has line-of-sight view between transceivers.

- *Licensing:* A major advantage of FSO over RF is that no telecommunication commission licensing or frequency allocating is required worldwide. This is because frequencies greater than 300GHz (less then 1mm in wavelength) are unregulated. In comparison latest GSM license treaty with Aria is over then two billion US dollars. In addition to the financial concerns in some urban areas or near airports it is very difficult and costly to obtain frequency allocation for microwave transmission.

- *Portability:* FSO terminals are portable and plug-and-play systems, which make them suitable for organizations like conferences and sport games (e.g. during 2000 Sydney Olympic Games FSO is applied). Another application area resulting from the portability is the 11th of September disaster in New York where FSO replaced the corrupted transmission lines.

- *Security:* FSO communication system as previously stated is based on the transmission of light in a confined beam, which is slightly diverges through the transmission path. This divergent structure of laser beam makes unauthorized detection, interception and jamming very difficult. The FSO systems are typically installed to guarantee the long-term line-of-sight stability so that passing vehicles or growing plants would not interfere with the beam. In addition beam disruption due to the possible intruders or hackers are immediately noticed even in very short-time periods by not only network specialist but also clients of the system. Because of its superior security, compared to RF-transmission, FSO is suitable for transfer of financial, legal, military or other sensitive information [9].

1.2.2 Disadvantages

FSO is a 'line-of-sight' technology with atmosphere as the transmission medium. Hence short and long-term atmospheric events such as rain, fog, snow, visibility, humidity and other obstacles (birds, trees, buildings etc.) affect the communication link.

- *Poor Weather:* Atmospheric events are the biggest obstacle in FSO communication links. Weather, which is dependent on the climate of region, is the main design constraint. Most of the atmospheric events are occurred in the first 16km of the earth layer, which is called Troposphere. During the link establishment in the Troposphere metrological incidents limit the achievable communication link distance. Commercial off-the-shelf FSO-systems have a maximal range of approximately 500m. Furthermore thick fog reduces link distance to only 200m or even less. Fog introduces the greatest challenge, as the water particles are small and dense enough the transmitted beam diffracted and totally extinct. Since the particles of rain and snowfall are large compared to the used wavelength, they affect the transmission less than fog [10, 11].

- *Physical Obstacles:* Unlike the competing RF transmission systems FSO link is severely affected by the physical medium of the channel. Dependent on the projected lifetime of the FSO system line-of-sight clearance is an important consideration. The growth of trees, construction of new buildings or even a single bird can block the transmitted beam. Hence future developments through the communication link path need to be carefully considered. Short-time link interruptions could be recovered by using different transmission protocols such as Ethernet and Token ring [4].

- *Building Movements:* Receiver and Transmitter alignment constraints dependent on building movements. Most of the buildings swing due to the wind, which causes the failure of the link.

- *Scintillation:* As the temperature of the atmosphere increases, different air molecules from various mediums (rooftops, ground etc.) heated in random manner which causes fluctuations in the refractive index of atmosphere in a time dependent structure which is called scintillation. Scintillation appear as power fluctuations in the receiver [12].

1.3 Thesis Background and Motivation

FSO communication systems despite their promising advantages are severely affected by weather events such as rain, fog etc. Hence, most of the researches focus on the availability of FSO systems under poor weather conditions. Major objective of these studies is to improve fade margin in order to realise error free links. Many communication techniques are applied so far to reduce link degradation: Multi-transmit apertures, RF license free back up, output power amplification, etc. All of the techniques applied in FSO result in an increase in overall system cost, which reduces advantage of FSO systems over other wireless technologies.

This master thesis has an alternative design approach to Free-space optical communication systems to reduce overall system cost without degrading system performance.

Figure 1.2 illustrates typical commercial FSO transceiver units applied in several FSO systems. Although the differences, transceivers use same basic approach for communication which is focusing the incoming beam by the receiving aperture to the detector. Receiver aperture is one of the main design constraints in FSO systems, which is mostly dependent on the divergence angle of the beam. Overall aperture size is selected in order to minimise displacement of the beam from the receiver. In most commercial applications receiver aperture is larger in diameter in contrast to transmit apertures.

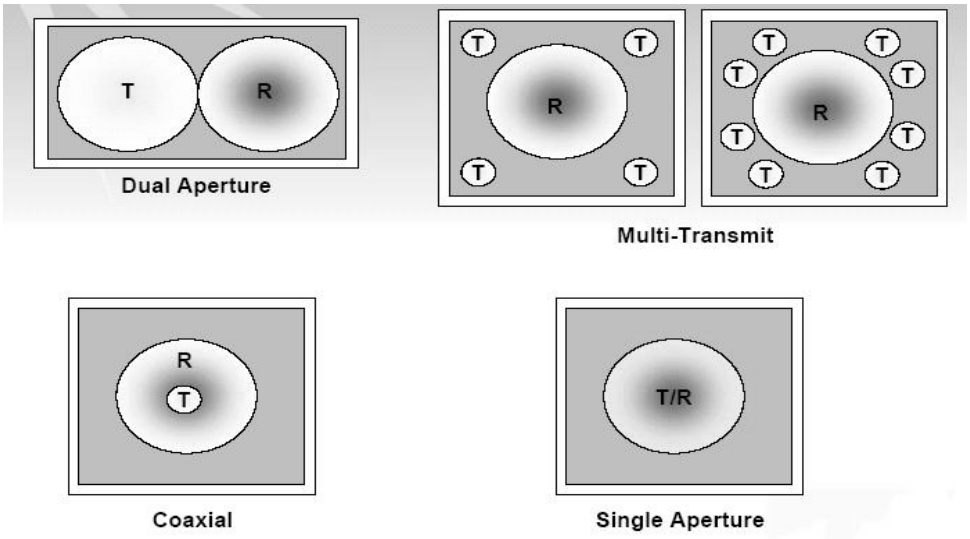

Figure 1.2. Typical FSO communication system transceivers.

Optical system cost in FSO is highly integrated with the aperture size, lens quality and the number of lenses. Most of the commercial FSO systems apply single lens solutions for reducing the overall system cost. Although single lens solution is less costly in comparison with the telescopic solution, lens price increases geometrically with the aperture size. Typical 150mm off-the-shelf Melles-Griot lens costs $2000 where 50mm lens costs only $100. While considering the entry-level low-speed (up to10Mbps) FSO systems, which are beginning from $4000, optical transceiver design is a provision.

The objective of alternative approach to free-space optical communication is to reduce optical system cost by using Fresnel lenses in place of bulk optic. Fresnel lenses may be applied at the receiver end of the link for focusing incoming beam to the detector with large apertures without insignificant rise in cost and weight. Fresnel optical technology has the following benefits:

- It is a robust low-cost technology without additional optical or electro-optical append to the system.
- The simplicity and low weight of the system implies easy and fast installation.
- Significant rise in displacement tolerance in contrast to the bulk optic systems.

1.4 The Outline of the Thesis Work

This master thesis is based on realisation of experimental FSO system. As a starting point theoretical characterisation of laser beam, bulk optic and Fresnel lenses are realised and laboratory tests are applied for the comparison of bulk optic systems with the Fresnel lens system. Secondly field tests are performed for either performance comparison of Fresnel lens and bulk optic or local atmospheric behaviour of interested area (Izmir Institute of Technology campus area). As a conclusion theoretical calculations and field tests are evaluated for determining the superiority of Fresnel lenses in place of bulk optic.

The report consists of five chapters. The first chapter is an introduction that also gives the motivation, description of the thesis and a brief history of the free-space optics.

The second chapter, Theory of Free-space communication, includes description of fundamental concepts regarding optics and the analysis of atmospheric attenuation and turbulence effects on system performance.

The third chapter, Free-space optical communication design tasks, describes the typical FSO transmitter and receiver design issues, equipment, performance considerations of the off-the-shelf systems.

The fourth chapter, Link budget and displacement analysis, includes the link budget of proposed FSO system with both bulk optic and Fresnel lens.

The fifth chapter, Results and conclusion, describes the performed laboratory and field tests. Background, measurement procedure, results and source of errors of test are elucidated.

Chapter 2

THEORY OF FREE SPACE OPTICAL COMMUNICATION

Free-space optical communication is based on the idea of using light beams for data transmission in an unguided medium. Like the Fiber-optic transmission systems FSO communication is the application of beam optics in unguided media. Although the wave nature of light prevents the existence of waves that are spatially localized and nondiverging, solution of the Helmholtz equation when the wavefront normals of the paraxial waves making small angles with the z axis exhibits the characteristics of an optical beam which called Gaussian beam. The basic approximation used in the analysis of light beam in the FSO communication systems is the Gaussian beam. Most lasers produce Gaussian beams that have point-source spatial qualities. For instance, single-mode lasers produce the narrowest of Gaussian beams, and the output of single-mode fiber coupled to such lasers is approximately Gaussian. Under the Gaussian beam assumption beam power is concentrated within a small cylinder surrounding the beam axis that permits the usage of light in communication systems.

2.1 Gaussian Beam

As mentioned in previous section Gaussian beam is one of the solutions of the Helmholtz equation. It is obtained from the paraboloidal wave by a simple transformation. Since the complex envelope of the paraboloidal wave (2.1.1) is a solution of the paraxial Helmholtz equation (2.1.2), a shifted version of it, with $z-\xi$ replacing z where ξ is a constant (2.1.3) is also a solution [13].

$$A(r) = \frac{A_1}{z}\exp(-jk\frac{\rho^2}{2z}), \rho^2 = x^2 + y^2 \tag{2.1.1}$$

$$\nabla_T^2 A - j2k\frac{\partial A}{\partial z} = 0, \tag{2.1.2}$$

$$A(r) = \frac{A_1}{q(z)}\exp(-jk\frac{\rho^2}{2q(z)}), \qquad q(z) = z - \xi \tag{2.1.3}$$

When ξ complex, equation (2.1.3) still remains a solution to the Helmholtz equation. Assuming ξ as $-jz_o$ where z_o is real then $q(z) = z + jz_o$.

To separate the amplitude and the phase from (2.1.3) we define $q(z)$ as $1/q(z)=1/(z + jz_o)$ That is,

$$\frac{1}{q(z)} = \frac{1}{R(z)} - j\frac{\lambda}{\pi w^2(z)}, \tag{2.1.4}$$

where $w(z)$ and $R(z)$ are measures of the beam width and wavefront radius of curvature. When we place the equation (2.1.4) to the equation (2.1.3) we obtain complex amplitude of the Gaussian beam (2.1.5). w_0 is the minimum value of the beam width called the beam waist at z=0 plane and z_0 is the Rayleigh range.

$$U(r) = A_0 \frac{w_0}{w(z)} \exp\left(-\frac{\rho^2}{w^2(z)}\right) \exp\left(-jkz - jk\frac{\rho^2}{2R(z)} + j\zeta(z)\right), \tag{2.1.5}$$

2.1.1 Beam Power

Optical power carried by the beam is confined in small radius of curvature. The total power of the beam is the integral of the optical intensity over a transverse plane where the intensity is defined by equation (2.1.6) [13].

$$I(\rho, z) = I_0\left(\frac{w_0}{w(z)}\right)^2 \exp\left(-\frac{2\rho^2}{w^2(z)}\right), \tag{2.1.6}$$

$$P = \int_0^\infty I(\rho, z) 2\pi\rho d\rho, \qquad \rho^2 = x^2 + y^2 \tag{2.1.7}$$

The ratio of the power carried within a circle of radius ρ_0 in the transverse plane at position z to the total power is,

$$\frac{1}{p}\int_0^\rho I(\rho, z) 2\pi\rho d\rho = 1 - \exp\left(-\frac{2\rho_0^2}{w^2(z)}\right), \tag{2.1.8}$$

2.1.2 Beam Width

The lateral boundaries of optical beams are not strictly defined as stated in equation (2.1.7). In practice different propagation models use Gaussian beams.

The commonly adopted definition of the beam width is the width at which the beam intensity has dropped to $1/e^2$ (13.5%) of its peak value (see figure 2.1). This definition applies for Gaussian beam and is appropriate for lasers operating in fundamental TEM_{00} mode [11].

Alternatively, the beam can also be characterized to where its radial amplitude declines to $1/e$ (36.8%) of its peak intensity at transverse plane. A third alternative is to characterize the beam by the full-width at half amplitude (FWHA), which is 58.9% for the Gaussian beam.

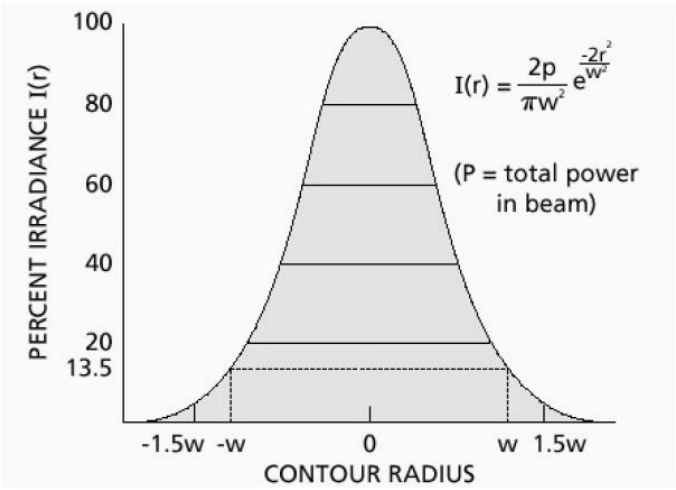

Figure 2.1. Gaussian profile of a TEM_{00} mode in free space. Note the beam radius w at the $1/e^2$ (13.5%) intensity level, r is the distance from beam center and w is the beam waist.

2.1.3 Beam Divergence

Optical beams propagate through the free-space with an angular spread defined as beam divergence. As stated previously much of the light power confined within a

small radius. Further the waist radius of the Gaussian beam is highly dependent on the longitudinal transmission plane where the equation (2.1.9) gives the relation [13].

$$w(z) = w_0\left[1+\left(\frac{z}{z_0}\right)^2\right]^{1/2}, \qquad (2.1.9)$$

The waist of beam increases gradually with increasing z, see Figure 2.2. For the values when the distance $z>>z_0$ the waist equation becomes,

$$w(z) = \frac{w_0}{z_0} z = \theta_0 z, \qquad (2.1.10)$$

θ_0, is the defined as $\frac{w_0}{z_0}$ and the $z_0 = \frac{w_0^2\pi}{\lambda}$ then $\theta_0 = \frac{\lambda}{\pi w_0}$, which is called divergence angle of the beam.

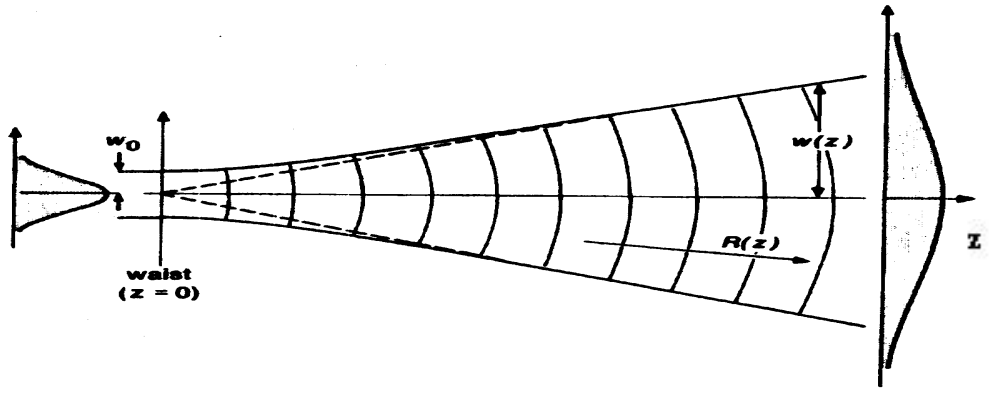

Figure 2.2. Gaussian Beam propagating through z-axes.

2.2 Fundamental Optics

As mentioned in preceding chapter free-space optical communication is a wireless technology that is mainly dependent on the optical behavior of the system. Unlike the RF systems antenna of the transceiver is replaced by the optical lens system in FSO systems. In this section a brief introduction to the optical properties of FSO communication is given that are referred in subsequent quotients.

2.2.1 Diffraction

Diffraction is a natural property of light beams occurred during the propagation. This phenomenon is a fundamental peculiarity that possesses a limitation to any optical system. Diffraction can be understood by considering the wave nature of light. Huygen's principle states that every point on the propagating wave front behaves like a point source resulted with secondary wavelets. Interference between these wavelets forms fringe pattern through transmission path. Diffraction is always present but can be omitted due the other drawbacks such as aberrations. When a lens, mirror or an entire optical system is designed to minimize aberration effects then these systems are called diffraction-limited [14,15].

2.2.2 Aberration

Theoretical analysis of lens systems for determining performance differs from the field observations. When ray tracing method is applied for comparison by using paraxial theory approximations it is seen that not all the rays passing through the predicted points. These deviations from the ideal solutions are called lens aberrations. Aberrations depend on the index of refraction, which is called Chromatic aberration and the shape of the lens, which is called Spherical Aberration.

The index of refraction of a material is a function of wavelength. Thus, light from different wavelengths will be refracted at different angles. Although the differences are occurred as a result of the alternating wavelengths FSO systems use monochromatic light that resulted with limited chromatic aberration [15].

Spherical aberration, which is the dominant aberration in FSO systems, is originated due the spherical shape of the lenses. With a spherical lens, the farther from the optical axis a ray enters the lens, the closer the lens it focuses. The distance along the optical axis between the interceptions of edge rays and the rays, which crossed nearly on the optical axis, called "*longitudinal spherical aberration*" (LSA). The height at which these rays intercept the paraxial focal plane is called "*transverse spherical aberration*" (TSA), see Figure 2.3 [15].

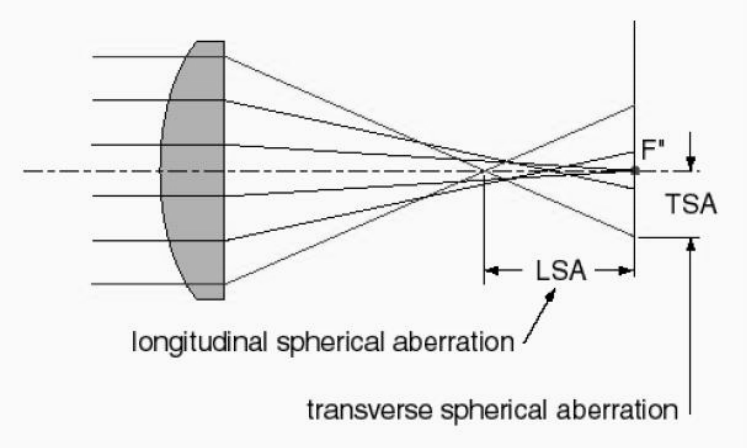

Figure 2.3. Spherical aberration of a lens.

2.2.3 Numerical Aperture and f-number of Lenses

The f-number, commonly denoted as f/#, is the ratio of the lens focal length to its effective diameter (clear aperture) [16].

$$F/\# = \frac{f}{\phi} \tag{2.2.1}$$

The f-number defines the angle of the cone of light leaving the lens under the assumption of uniformly illumination of positive focal length lens by collimated light, see Figure 2.4.

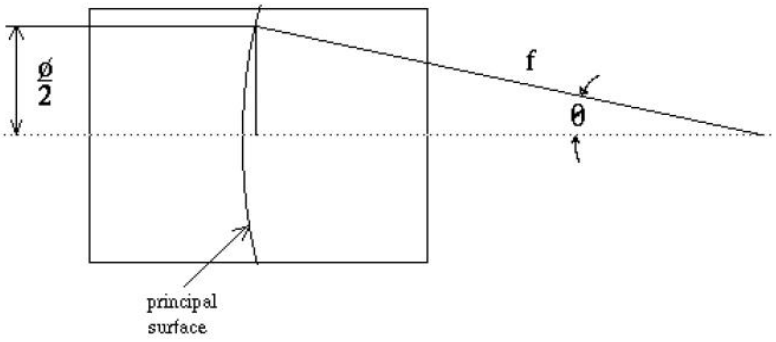

Figure 2.4. Numerical aperture and f/#.

The other commonly used term to define this angle is the Numerical aperture (NA). The numerical aperture is the sine of the angle, which is the angle between

marginal ray and the optical axis [16]. Referring to the Figure 2.5 and simple trigonometry, it can bee seen that:

$$NA = \sin\theta = \frac{\phi}{2f} \tag{2.2.2}$$

or

$$NA = \frac{1}{2f/\#} \tag{2.2.3}$$

2.2.4 Spot Size

Spot size is theoretically defined as the minimum achievable beam diameter at the transmission path. Equation 2.1.9 states the relation between the beam waist and z (longitudinal path). When z=0 then the beam waist take its minimum value w_0 and the waist diameter is called the *spot size*. Spot size of a lens varies according to the optical characteristics of the lens material. The smallest possible spot size dictated by diffraction and thereby defined as [16]:

$$d = K\lambda f/\# \tag{2.2.4}$$

where d is the diameter of the focused spot produced from plane wave illumination and λ is the wavelength. As stated spot size is determined by the f-number of the lens and the wavelength. For example, the spot size in the case of a diffraction-limited lens will be twice as large using 1550nm compared to 785nm. The K is a constant dependent on the pupil illumination, which is 2.44 when the illumination is uniform.

To verify whether the pupil illumination can be approximated as uniform when Gaussian output beam is present, truncation ratio introduced, T:

$$T = \frac{D_b}{D_t} \tag{2.2.5}$$

D_b is the Gaussian beam diameter measured at the $1/e^2$ intensity point and D_t is the limiting aperture diameter of the lens. If $T>2$, uniform illumination can be assumed and then the spot size under uniform illumination assumption can be determined without

any truncation. If *T=1* the spot profile will be a hybrid between uniform and Gaussian distribution. When *T=0.5* the spot intensity profile approaches a Gaussian distribution. Calculations of the spot size for truncation ratios less than two (*T<2*) requires that K be evaluated. This is done, at the $1/e^2$ intensity point, applying the formula [15].

$$K_{1/e^2} = 1.6449 + \frac{0.6460}{(T-0.2816)^{1.821}} + \frac{0.5320}{(T-0.2816)^{1.891}} \tag{2.2.6}$$

For example when *T=1* then K_{1/e^2} becomes 1.83.

Instead of diffraction when spherical aberrations are dominant in lens structure (e.g. commonly when using plano-convex lens) then spot size is stated by aberrations. Equation 2.2.7 shows the spot size of plano-convex lens when monochromatic and approximately incident plane wave is the case.

The spot size due to spherical aberration is [15]:

$$d = \frac{0.067 f}{f/\#^3} \tag{2.2.7}$$

Since, in the case of one spherical lens, the diffraction increases and aberration decreases with increasing f-number, determining optimum system performance often involves finding a point where the combination of these factors has a minimum effect [15].

2.2.5 Fresnel Reflections

Incident light propagating through transparent surfaces experiences a reflection at an interface between two media having different refractive indices is named Fresnel reflection. For a normal wave, the fraction of reflected incident power is given by the equation [17].

$$R = \frac{(n_1 - n_2)^2}{(n_1 + n_2)^2} \tag{2.2.8}$$

where R is the reflection coefficient and n_1, n_2 are the refractive indices of two media respectively. With $n_1 = 1$ (refractive index for air) and $n_2 = 1.5$ (refractive index for the glass of interest) this yields:

$$R = \frac{(1-1.5)^2}{(1+1.5)^2} = 0.04$$

Thus, 4 % transmission loss exists on every glass-air interface transition due to the Fresnel reflections.

2.2.6 Field-of-view

In free-space optical communication, which is a light-off-sight technology as stated in prior sections, optical receiver alignment takes much attention in system performance calculation, commonly know as field-of-view (FOV).

- *Receiver unit one lens:* Apart from the spot size, the tolerance for a receiver with one lens depends on the focal length of the lens. A simple model for the FOV of the receiver can be found by geometrical considerations from Figure 2.5 [16]:

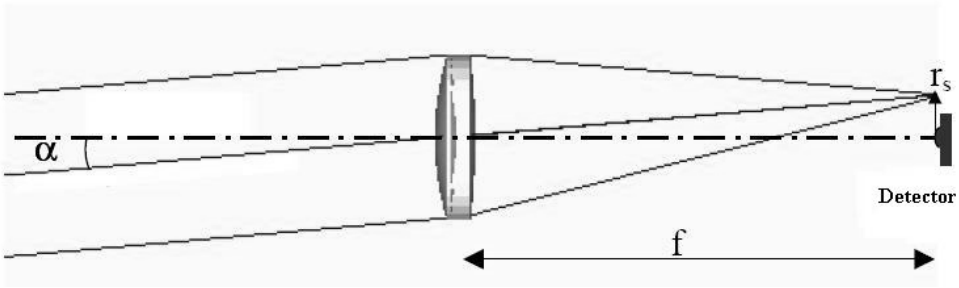

Figure 2.5. Receiver alignment tolerances.

$$\alpha < \tan^{-1} \frac{r_s}{f} \qquad (2.2.9)$$

where,

2α = Field of view (FOV),

r_s = Tolerable spot center displacement defined at 3dB loss,

f = Lens focal length.

- *Receiver unit with multiple lenses:* To calculate the FOV for a receiver with multiple lenses ABCD transfer matrix can be used to describe the beam propagation through the lens system. The ABCD matrix for propagation through a (concave or convex, see Figure 2.6) thin lens and through the space between optical components can be written in the form [13]:

Thin lens

$$\begin{bmatrix} A & B \\ C & D \end{bmatrix} = \begin{bmatrix} 1 & 0 \\ -\frac{1}{f} & 1 \end{bmatrix} \tag{2.2.10}$$

Free space

$$\begin{bmatrix} A & B \\ C & D \end{bmatrix} = \begin{bmatrix} 1 & d \\ 0 & 1 \end{bmatrix} \tag{2.2.11}$$

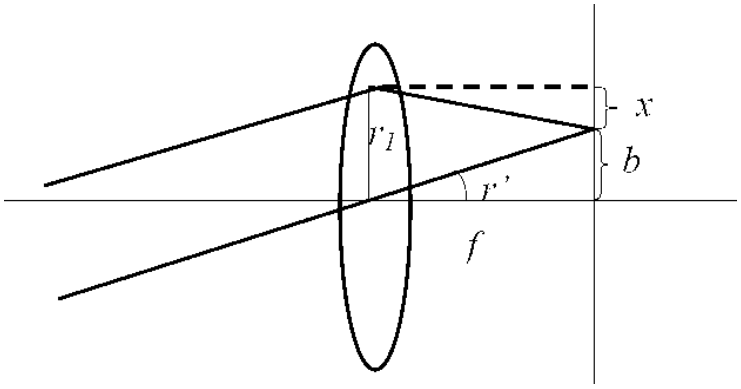

Figure 2.6. Propagation through a thin lens.

Transmitted signal through thin lens is characterized as follows:

$$\begin{bmatrix} r_2 \\ r_2' \end{bmatrix} = \begin{bmatrix} A & B \\ C & D \end{bmatrix} \begin{bmatrix} r_1 \\ r_1' \end{bmatrix} = \begin{bmatrix} 1 & 0 \\ -\frac{1}{f} & 1 \end{bmatrix} \begin{bmatrix} r_1 \\ r_1' \end{bmatrix} = \begin{bmatrix} r_1 \\ r_1' - \frac{1}{f} r_1 \end{bmatrix}$$

$$b = r_1' . f, \quad x = r_1 - b$$

$$r_2' = -\frac{x}{f} = -\frac{r_1 - b}{f} = \frac{b}{f} - \frac{r_1}{f} = r_1' - \frac{r_1}{f}$$

$$q_2 = \frac{Aq_1 + B}{Cq_1 + D} = \frac{q_1}{-\frac{q_1}{f} + 1}, \quad where \quad \frac{1}{q_{1(2)}} = \frac{1}{R_{1(2)}} - j\frac{\lambda}{\pi w_{1(2)}}, (equation \quad 2.1.4)$$

Transmission through free space is:

$$\begin{bmatrix} r_2 \\ r_2^{'} \end{bmatrix} = \begin{bmatrix} 1 & d \\ 0 & 1 \end{bmatrix} \begin{bmatrix} r_1 \\ r_1^{'} \end{bmatrix} = \begin{bmatrix} r_1 + dr_1^{'} \\ r_1^{'} \end{bmatrix}$$

The propagating matrix of the receiver system is found by multiplication of each ABCD (abbreviated as A) matrix:

$$\overline{r_n} = A_n A_{n-1} \ldots\ldots A_2 A_1 \overline{r_1} \tag{2.2.12}$$

$$r_n = A r_1^{'} = A \tan\alpha$$

$$Thus, \quad FOV \quad is \quad \alpha < \tan^{-1} \frac{r_n}{A} \tag{2.2.13}$$

2.3 Link Degradation

Free-space optical communication systems are highly integrated with the optical losses of transceiver and atmospheric degradation effects of the channel. In this section, link degradation effects in FSO communication are depicted. Figure 2.7 shows the factors that may cause power losses during transmission [11,13].

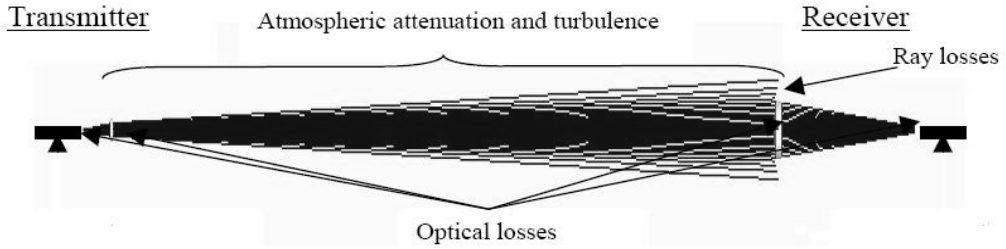

Figure 2.7. Factors that have effect on the link performance.

2.3.1 Optical Losses

In every case of glass-to-air or air-to-glass transitions, there are losses due to the Fresnel reflection [17]. As mentioned in previous sections Fresnel reflections dependent on the indices of the materials and calculated power loss is 4% for the standard lenses

on every glass-air transition. Figure 2.8 shows the reflected power percentage change due to the index change.

.

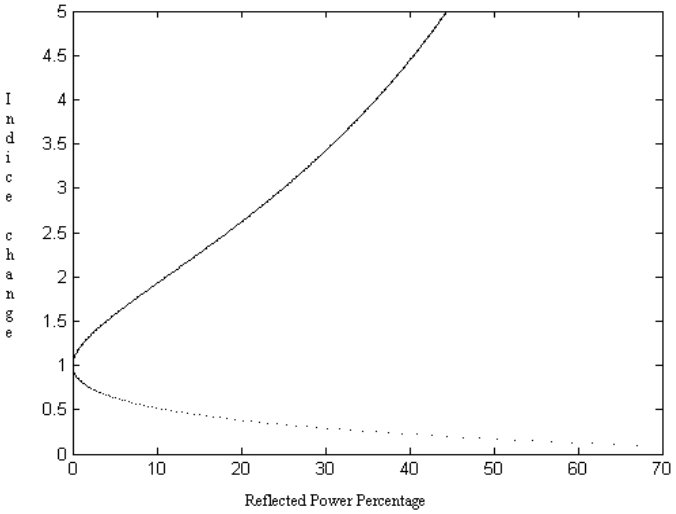

Figure 2.8. Fresnel reflection.

To decrease the Fresnel reflections, the lens surface may be anti-reflection (AR) coated and total reflection reduced to 0.1% [18].

2.3.2 Ray Losses

As stated in previous sections that the beam power carried through transmission medium is the integral of the optical intensity over a transverse plane. (Equation 2.1.7) Thus total beam power is defined as:

$$P = \int_0^{\infty} I(\rho, z) 2\pi\rho d\rho$$

$$\textit{which} \quad \textit{gives} \qquad (2.3.1)$$

$$P = \frac{1}{2} I_0 (\pi w_0^2),$$

The result is independent of z, as expected. Hence the beam power is one-half the peak power intensity times the beam area. Since beams are described by their power P, it is useful to express I_0 in terms of P from (2.1.6) and (2.3.1)

$$I_0(\rho, z) = \frac{2P}{\pi w^2(z)} \exp\left[-\frac{2\rho^2}{w^2(z)}\right], \tag{2.3.2}$$

In Free-space optical communication systems collected power is dependent on the radius of the receiver lens and the beam radius at the receiver unit, see equation 2.3.3.

$$F_s = 10 \log \frac{p_{receiver}}{P_{total}}$$

$$\frac{P_{receiver}}{P_{total}} = \frac{1}{P_{total}} \int_0^R I(\rho, z) 2\pi d\rho = 1 - e^{-\frac{2R^2}{w^2(z)}} \Rightarrow F_s = 10 \log\left(1 - e^{-\frac{2R^2}{w^2(z)}}\right) \tag{2.3.3}$$

where,

z = Link distance [m]

F_s = Ray losses [dB]

$P_{receiver}$ = Power hitting the first receiver lens

P_{total} = Total beam power at z

R = Lens radius [m]

I_0 = Output optical intensity

$I(\rho, z)$ = Optical intensity

w(z) = Beam radius (at $1/e^2$)

ρ = Radial coordinate with respect to the beam axis

Equation 2.3.3 shows that the received power highly dependent on the beam waist at distance z. To have an appropriate value on the beam waist through the communication channel transmitter lens could be adjusted. When light propagates through air, diffraction spreads the laser beam transversely. Even if the laser beam wavefront collimated, it would quickly acquire curvature and begin spreading in accordance with:

$$w(z) = w_0 \left(1 + \frac{\lambda z}{\pi w_0^2}\right)^2, \tag{2.3.4}$$

For example, if the wavelength is 1550nm and the transmitter lens radius (w_0) is one centimeter, then the beam radius would be 3cm after 400m of propagation. Figure 2.11 compares the ray losses for lenses with a diameter of 50mm and 100mm respectively. It is seen that the difference between the two receiver lenses approaches 6dB (a factor of 4) as the beam diameter increases.

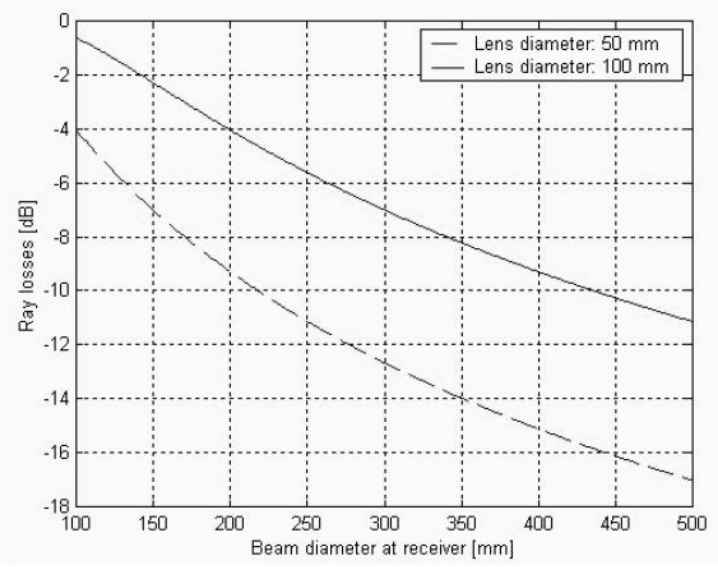

Figure 2.9. Ray losses vs. beam diameter for different lenses.

2.3.3 Ray Losses Including Errors of A Misdirected Transmitter

In prior section ray losses in optical free-space communication systems are considered during the propagation between transmitter and receiver. If the laser beam is misdirected which is the displacement of the intensity maximum from the receiver lens, the loss will increase.

The optical intensity is a function of the axial and radial coordinates z, ρ and the beam waist as defined in equation 2.1.6. Beam waist naturally occurs at the midplane of a symmetric confocal cavity. Thus, the beam waist can be well approximated by the transmitter lens radius. (In the case of full filled lens) [13].

In the case of constant beam intensity over the receiver then the beam power becomes:

$$P_{receiver} = \pi R^2 I_0 \left(\frac{w_0}{w(z)} \right)^2 \exp\left(-\frac{2\rho^2}{w^2(z)} \right) \qquad (2.3.5)$$

Since the total beam power is given by equation 2.3.1. The ratio of the power carried within the receiver aperture to the total power becomes:

$$\frac{p_{receiver}}{P_{total}} = \frac{\pi R^2 I_0 \left(\frac{w_0}{w(z)}\right)^2 \exp\left(-\frac{2\rho^2}{w^2(z)}\right)}{\frac{1}{2} I_0 \pi w_0^2} = \frac{2R^2 \exp\left(-\frac{2\rho^2}{w^2(z)}\right)}{w^2(z)} \tag{2.3.6}$$

2.3.4 Atmospheric Effects on Laser Beam Propagation

As the free-space optical communication systems transmitted data by modulated laser light through the atmosphere, they are severely affected by the atmospheric phenomenons such as wind, rain, snow, fog etc. Atmospheric effects on laser beam propagation can be broken into two categories: attenuation of the laser power and fluctuation of laser power due to the atmospheric turbulence. Attenuation consists of absorption and scattering of the laser beam by the different aerosols and gaseous molecules in the atmosphere. Atmospheric turbulence (scintillation) occurs because of the small-scale variations on the index of refraction of transmission medium. These effects cause the degradation of the laser beam such as beam spreading, beam wander.

2.3.4.1 Atmospheric Attenuation

During the transmission of the laser beam through air, it is exposed to attenuation depending on the weather conditions. The equation of the laser transmission in air is described by Beer-Lambert's law as [4,11]:

$$\tau(R) = \frac{p(R)}{P(0)} = \exp(-\sigma R) \tag{2.3.7}$$

where $\tau(R)$ = transmittance at range R,

P(R) = laser power at R,

P(0) = laser power at the source, and

σ = Attenuation or total extinction coefficient (per unit length).

Typical attenuation coefficients are clear air = 0.1 (0.43dB/km), haze = 1 (4.3dB/km), and fog = 10 (43dB/km).

The total attenuation coefficient can be divided into four parts:

$$c = \alpha_m + \alpha_a + \beta_m + \beta_a$$

where α_m = Molecular absorption coefficient

α_a = Aerosol absorption coefficient

β_m = Molecular or Rayleigh scattering coefficient

β_a = Aerosol or Mie scattering coefficient.

The attenuation coefficient has contributions from absorption and scattering by different aerosols and gaseous molecules. Since free-space optical communication wavelengths are chosen to fall outside the transmission window of deep absorption spectra, (Typically 785nm, 1550nm) then the effects of scattering, therefore dominates the total extinction coefficient, see Figure 2.10.

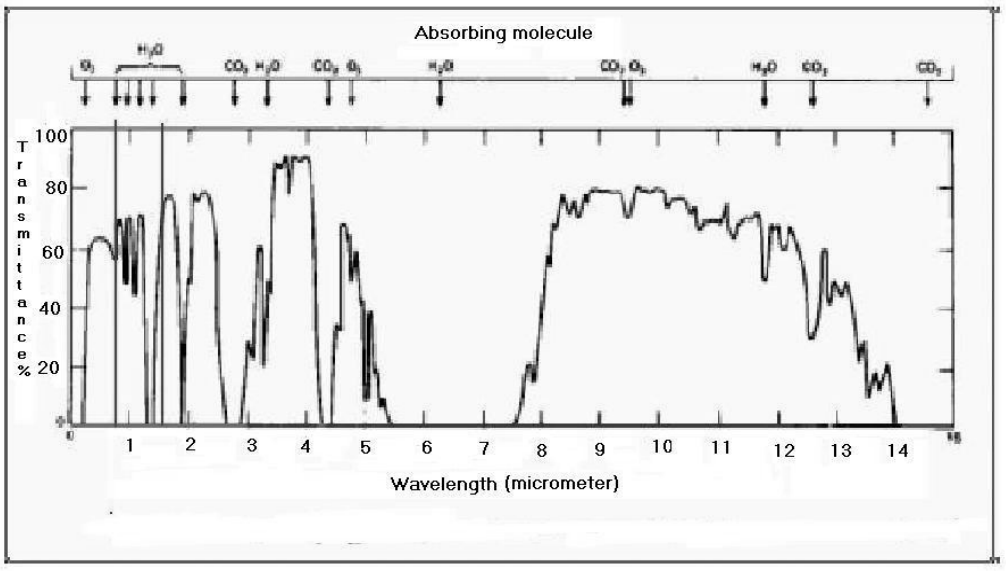

Figure 2.10. Atmospheric transmission window versus wavelength.

The type of scattering is determined by the size of the particular atmospheric particle with respect to the transmission wavelength, which is determined by dimensionless number α called size parameter.

$$\alpha = \frac{2\pi r}{\lambda} \tag{2.3.8}$$

where r = radius of the scattering particle,

λ = laser wavelength.

Table 2.1 shows the change of the radius of scattering particles in different atmospheric conditions and their corresponding size parameter in two distinct wavelengths (785nm, 1550nm) [19].

Table 2.1. Typical atmospheric scattering particles.

Type	Radius (μm)	Size Parameter α	
		785 nm	1550 nm
Air Molecules	0.0001	0.0008	0.0004
Haze particle	0.01 - 1	0.08 - 8	0.04 - 4
Fog droplet	1 to 20	8 - 160	4 - 80
Rain	100 to 10000	800 to 80000	400 to 40000
Snow	1000 to 5000	8000 to 40000	4000 to 20000
Hail	5000 to 50000	40000 to 800000	20000 to 400000

The size parameters of atmospheric scattering particles for corresponding wavelengths of 785nm and 1550nm are plotted in Figure 2.13, demonstrating the regions for Rayleigh, Mie, and non-selective or geometric scattering with the relation to the power law of attenuation coefficient [19].

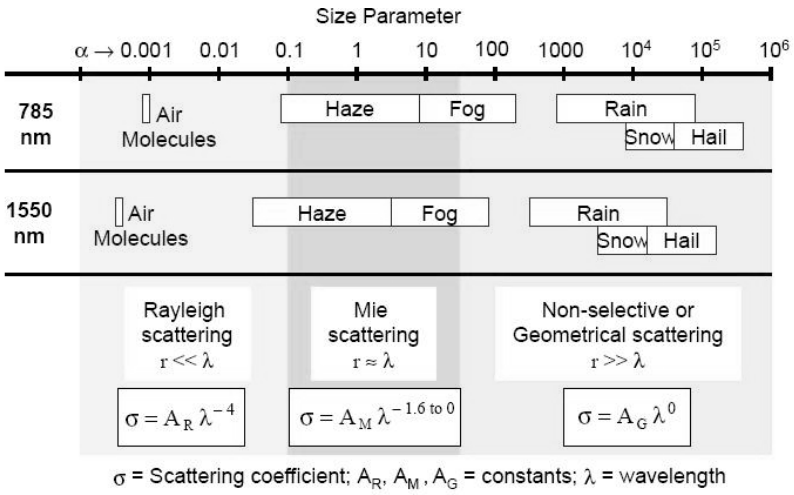

Figure 2.11. Size parameters of atmospheric scattering particles in Table 2.1.

From figure 2.11, Rayleigh scattering occurs when the atmospheric particles (mostly gaseous molecules in the atmosphere) are much smaller than the wavelength of the laser beam. Rayleigh scattering is dependent to the wavelength of interest with a power of –4, which highly decreases its effect on total attenuation coefficient.

As the particle size approaches the laser wavelength, Mie scattering occurred by haze and small fog particles dominate the total attenuation coefficient. For Mie scattering, the exponent in the power law dependence on wavelength is varies from 0 to 1.6.

The third generalized scattering regime occurs when the atmospheric particles much larger than the laser wavelength. As the size parameters increases above value of 50 then scattering particles behave in a fashion where geometric optics describes the scattered radiation of laser beam. Raindrops, snow, hail, cloud droplets, and heavy fogs will geometrically scatter laser beam. This regime is called non-selective because there is no dependence of the attenuation coefficient on laser wavelength (power law exponent is zero).

To calculate total atmospheric attenuation coefficient σ each scattering size particle distributions contributed from different weather conditions are summed:

$$\sigma_{scat} = \sum_i n_i Q_i \pi r_i^2 \tag{2.3.9}$$

where n_i = distribution or concentration of the *i*th particle

Q_i = scattering efficiency of the *i*th particle,

r_i = radius of the *i*th particle.

The scattering efficiency Q is defined as the scattering cross-section normalized by the particle cross-sectional surface:

$$Q = \frac{C}{2\pi r} \tag{2.3.10}$$

where r = radius of the particle and

C = scattering cross-section which is dependent on the size parameter.

To calculate equation 2.3.9 scattering particle size distribution at any time window has to be driven from experimental observations, which is unfortunately not readily available data in most rural or urban areas. Hence more useful form of equation 2.3.8 needed to be calculated.

Since the scattering efficiency is a function of the size parameter, it is also a function of r/λ. Therefore equation 2.3.9 generalized to the form:

$$\sigma = A\lambda^{-q} \tag{2.3.11}$$

where A and q are constants determined by the size and distribution of the scattering particles [11]. An expression for A can be derived from the definition of visual range and q from experimental data [20]:

$$\sigma = \frac{3.91}{V}\left(\frac{\lambda}{550nm}\right)^{-q} \tag{2.3.12}$$

where V = Visibility in kilometers

λ = Wavelength in nanometers

q = The size distribution of the scattering particles

= 1.6 for high visibility (V< 50 km)

= 1.3 for average visibility (6km < V < 50 km)

= $0.585V^{1/3}$ for low visibility (V < 6 km)

Table 2.2 shows a theoretical comparison of the attenuation between the laser wavelengths 785nm and 1550nm using the equations 2.3.7 and 2.3.12. Note that longer wavelengths have better transmission.

Table 2.3 shows an experimental data obtained by Terralink8-155, which operates in 785nm wavelength range, during different weather conditions. Experimental results satisfy the empirical formula given in equation 2.3.12.

Table 2.2. A table of atmospheric losses (in dB/km) as a function of visibility.

Visibility (km)	dB/km 785 nm	dB/km 1550 nm	Weather
0.05	315	272	Fog
0.2	75	60	
0.5	29	21	
1	14	9	
2	7	4	Haze
4	3	2	
10	1	0.4	Clear
23	0.5	0.2	

Table 2.3. Terralink8-155 performance under different conditions with visibility decibel loss per kilometer attenuation and maximum link range.

Weather condition	Precipitation mm/hr	Visibility	dB loss/ km	TerraLink 8-155 Range
Dense fog		0 m		
		50 m	-315.0	140 m
Thick fog		200 m	-75.3	460 m
Moderate fog		500 m	-28.9	980 m
Light fog	Cloudburst 100	770 m	-18.3	1.38 km
		1 km	-13.8	1.68 km
Thin fog	Heavy rain 25	1.9 km	-6.9	2.39 km
		2 km	-6.6	2.79 km
Haze	Medium rain 12.5	2.8 km	-4.6	3.50 km
		4 km	-3.1	4.38 km
Light Haze	Light rain 2.5	5.9 km	-2.0	5.44 km
		10 km	-1.1	6.89 km
Clear	Drizzle 0.25	18.1 km	-0.6	8.00 km
		20 km	-0.54	8.22 km
Very Clear		23 km	-0.47	8.33 km
		50 km	-0.19	9.15 km

Snow

Although the Table 2.3 states that the equation 2.3.12 applicable for calculation of atmospheric attenuation coefficient in 785nm range, empirical data indicates there is no wavelength dependence for atmospheric attenuation between 785nm and 1550nm during rain and snow, see figure 2.11. To investigate the attenuation coefficient

depending on absorption and scattering in molecules so called atmospheric windows versus wavelength computer simulation software Modtran 4.0 is applied under different weather conditions, see Figure 2.12 and 2.13. It can be noted from the simulation results that the transmittance in fog is slightly better for 785nm than 1550nm. Thus simulation results agrees with the empirical data on contrary opposed to the equation 2.3.12 which is the case because the Modtran considers all four parts of the total extinction coefficient.

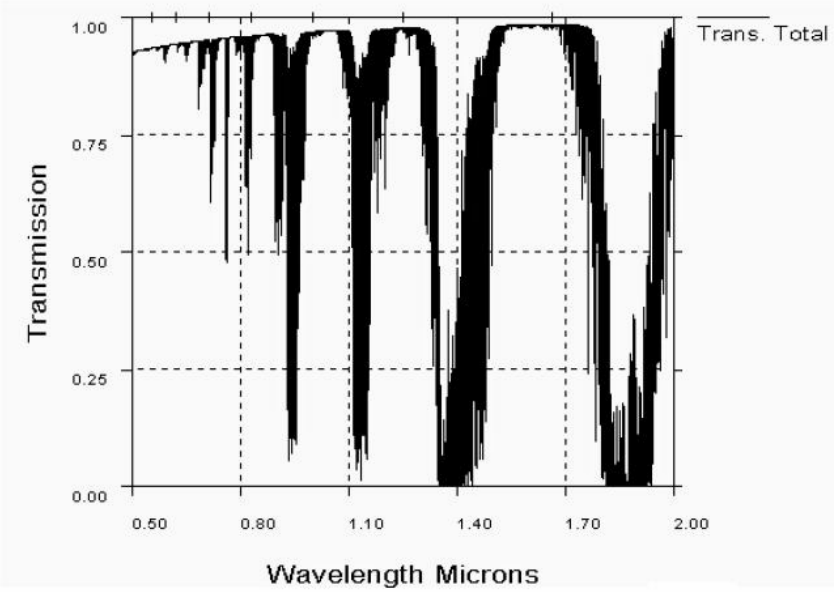

Figure 2.12. Transmission simulation in Modtran 4.0. Good visibility (23 km).

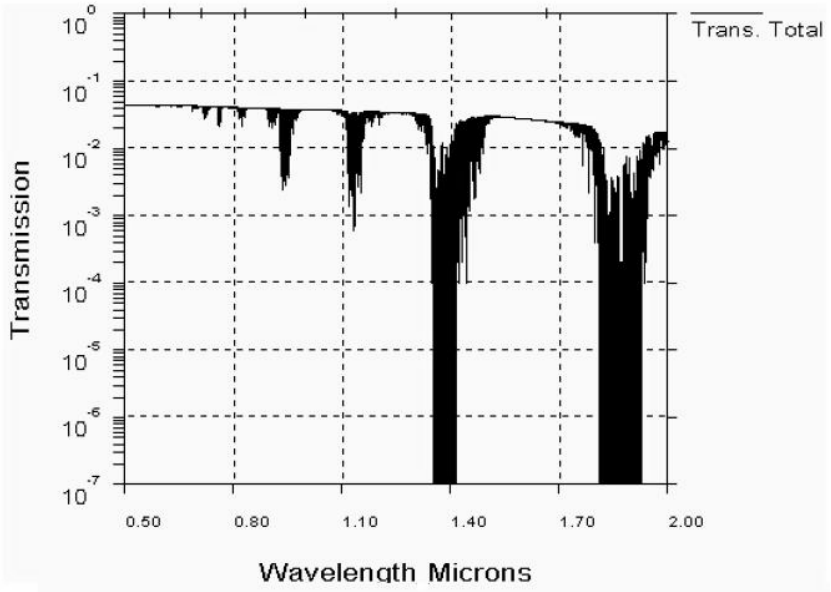

Figure 2.13. Transmission in fog. Poor visibility (0.5km).

For full filling the misleading results obtain from equation 2.3.12 an alternative equation proposed for the case of transmission under fog [11].

$$\sigma = \frac{3.91}{V}\left(\frac{\lambda}{550nm}\right)^{-q} \qquad (2.3.13)$$

where σ = atmospheric attenuation (or scattering) coefficient

V = visibility (in km)

λ = wavelength (in nm)

q = the size distribution of the scattering particles

= 1.6 for high visibility (V > 50km)

= 1.3 for average visibility (6 km < V < 50 km)

= 0.16V+0.34 for haze visibility (1 km < V < 6 km)

= V-0.5 for mist visibility (0.5 km < V < 1 km)

= 0 for fog visibility (V < 0.5 km)

Table 2.4 shows the results obtained from the equation 2.3.13, which clarifies the results of the computer simulations [11].

Table 2.4. Atmospheric losses (in dB/km) as a function of visibility for 785nm and 1550nm calculated using the new expression for q.

Visibility (km)	dB/km 785 nm	dB/km 1550 nm	Weather
0.05	340	340	Fog
0.2	85	85	
0.5	34	34	
1	14	10	
2	7	4	Haze
4	3	2	
10	1	0.4	Clear
23	0.5	0.2	

2.3.4.2 Atmospheric Turbulence

Free-space optical communication system performance is highly degraded by the structure of atmosphere and the weather events like fog, snow etc. as stated in preceding sections. Furthermore turbulence so called scintillation, which is originated

from the heat, and wind cause variations in the spatial intensity distribution of the laser beam. The theory, which is used to describe the effects of atmospheric turbulence on laser beam propagation, was developed for general electromagnetic propagation through random media [11]. Atmospheric turbulence, from wind or from temperature differences between the ground and the air, produce temporary pockets of air with slightly different temperature, density, and index of refraction. These air pockets (turbulence cells) are continuously changing in size due to the change in variations and also their energy redistributed to other cells as they mixed. The size of turbulence cells normally ranges from a few millimeters to a few meters. A laser beam wavefront propagating through these cells are deformed and distorted since air pockets act as a small lenses and prisms. If the size of cells smaller in comparison to the beam diameter then constructive and destructive interference causes rapid fluctuations in laser power at the receiver end, which is similar to the twinkling of a distant star. In addition when these cells larger than the beam diameter, the whole laser beam bends which is called beam wandering. These effects are illustrated in Figure 2.14 and 2.15.

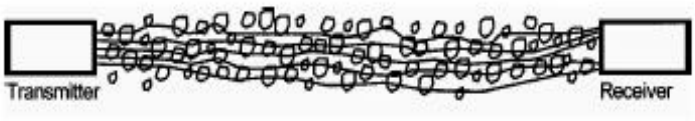

Figure 2.14. Scintillation in beam intensity due to the turbulent cells that are smaller than beam diameter.

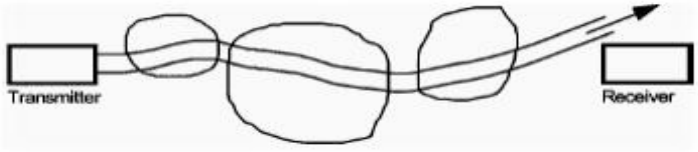

Figure 2.15. Laser beam wander due to the turbulent cells that are larger than beam diameter.

The theoretical formalism of atmospheric turbulence is complicated. To define the turbulence occurred as refractive index fluctuation of the laser power several models are proposed. One popular model is the Kolmogorov theory [21].
To express the turbulence; the refractive index change defined as:

$$n(\vec{r},t) = n_0 + n_1(\vec{r},t) \qquad (2.3.14)$$

where n_0 = the average index

n_1 = fluctuation component induced by spatial variations.

The correlation function of n_1 is defined as:

$$\Gamma_{n_1}(\vec{r_1},t_1;\vec{r_2},t_2) = E\left[n_1(\vec{r_1},t_1).n_1(\vec{r_2},t_2)\right] \tag{2.3.15}$$

Setting $t_1 = t_2$ in equation 2.3.15 then the correlation function becomes $\Gamma_{n_1}(\vec{r_1},\vec{r_2})$, which describes the spatial coherence of the refractive index. To study coherence of refractive index wavenumber spectrum $\phi_n(k)$ is defined to be spatial function $\Gamma_{n_1}(\vec{r_1},\vec{r_2})$. Kolmogorov theory accurately defines the wavenumber spectrum:

$$\phi_n(\vec{k}) = 0.033C_n^2 k^{-11/3}, \tag{2.3.16}$$

The level of turbulence measured with C_n^2 which is the wavenumber spectrum structure parameter. A high level of turbulence is found close to the ground during sunny summer days. While the turbulence is comparably low during dusk and dawn when the temperature change is low and the wind is gentle [16].

Figure 2.16 shows measurements of a typical of C_n^2 during a summer day [23]. Clouds passing by and interrupting the sun heating can explain sudden changes during daytime.

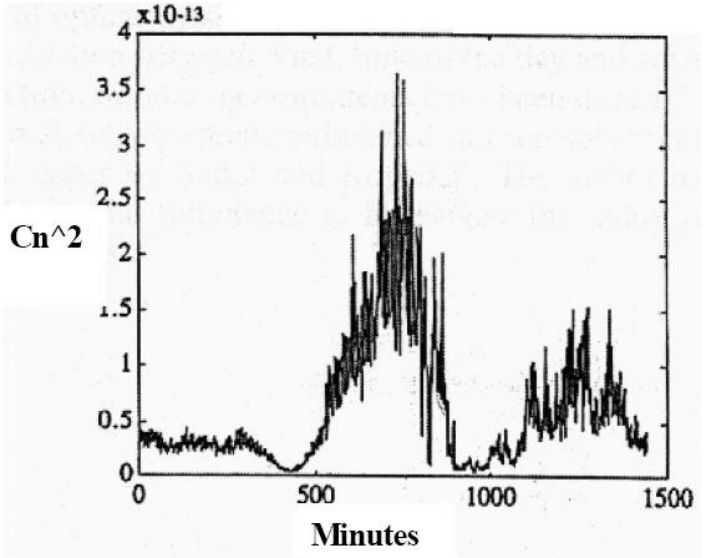

Figure 2.16. The variations of C_n^2 over 24 hours measured from midnight. Typical summer day at about 1.5 meter above ground.

C_n^2 is an altitude dependent parameter where it vary from $10^{-13} m^{-2/3}$ for strong turbulence to $10^{-17} m^{-2/3}$ for weak turbulence channels near ground (z < 18.5m). In hot summer days close to ground, the C_n^2 might reach $10^{-12} m^{-2/3}$. The altitude decrease of C_n^2 is modeled as [16]:

$$C_n^2(h) = C_n^2(1) h^{\alpha} \tag{2.3.17}$$

where h = altitude (m)
$C_n^2(1)$ = value at 1 meter

$$\alpha = \begin{cases} -4/3 & during \quad daytime \\ -2/3 & during \quad nighttime \end{cases}$$

If the scintillation due to the turbulence are strong, they may cause fading. Fading occurs when the signal power diminishes below a certain threshold value. This may give rise to bit errors.

The probability that the irradiance (I) falls below the threshold value I_T is [22]:

$$p(I \le I_T) = \frac{1}{2}\left(1 + erf\left(\frac{\frac{1}{2}\sigma_I^2(\rho, z) + 2\frac{\rho^2}{w_e^2} + \ln\left(\frac{I_T}{\langle I(0,z)\rangle}\right)}{\sqrt{2}\sigma_I(\rho, z)}\right)\right) \tag{2.3.18}$$

where σ_I^2 = normalized irradiance variance

ρ = radial coordinate with respect to the beam axis (ρ = 0 at the beam axis)

w_e = beam radius after turbulence influence

z .= link distance

erf(X) is the error function for each element of X, where X must be real. The error function defined as:

$$erf(X) = \frac{2}{\sqrt{\pi}} \int_0^X e^{(-t^2)} dt$$

and where a relative threshold can be defined as:

$$F_T = 10\log\left(\frac{\langle I(0,z)\rangle}{I_T}\right) \qquad [dB] \tag{2.3.19}$$

Figure 2.17 shows the probability of fading as a function of the threshold F_T.

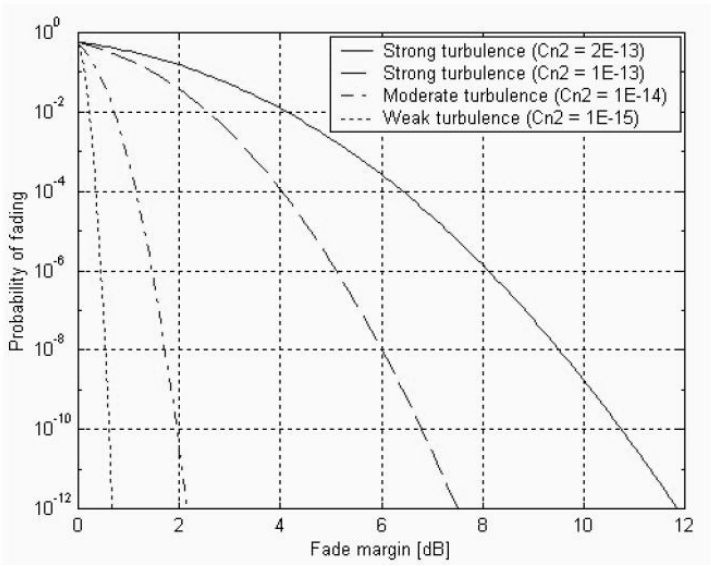

Figure 2.17. The probability of fading as a function fade margin, based on the threshold value needed for different levels of turbulence.

Throughout the chapter theoretical overview of FSO system is given with the link degradation effects. As stated FSO systems are severely affected by atmospheric attenuation and ray losses. Atmospheric events are dependent to the region where the link is installed. Visibility measure, which is related to the general climate of the district, designates the availability of the link distance. In addition scintillation effects introduces fades to the transmitted signal generated from the short-term wind and heat variations. Furthermore ray loss is the other major problem in FSO communication. As mentioned previously laser beam power is dissipated through air depending to the divergence angle.

Chapter 3

FREE-SPACE OPTICAL COMMUNICATION DESIGN TASKS

FSO technology arises as an alternative in communication market to the insatiable growth of the bandwidth demand in the marketplace. Several key factors are bringing FSO systems into the carrier space as a means of broadband access. One is the low-cost and the other is the ease of installation. Despite the increasing interest in the marketplace there are many near-hurdles for FSO products. This chapter's intention is to describe system design issues of commercial FSO communication system including the investigation of alternative technologies.

3.1 Free-Space Optical Communication Subsystems

Figure 3.1 illustrates the major subsystems in a complete free-space optical communication system. Typical FSO system bases on the transmission of modulated data through the transmission path via the transmitter laser and optics. Although the figure 3.1 shows the internal modulation scheme, some systems use external modulation and some others omit the electronic system and realise fiber-to-fiber coupled systems [5,6,16]. In typical FSO system main design challenges are the realisation of the optical system and the selection of transmission laser dependent on the requested bandwidth. Optical apertures in FSO systems can have different variety of forms and variety functions. Although the transmit and receive telescopes are illustrated as separate optical apertures in Figure 3.1, there are several other configurations possible which perform single apertures in place of all two functions thereby saving cost, weight and size. On the transmit side, important aspects of the optical systems are size and quality of the aperture. Size determines the maximum laser flux permitted and quality determines the minimum divergence angle obtainable. On the receiver side, the most important aspects are the aperture size and the f-number. The aperture size determines the amount of light collected and the f-number determines the detector's field of view. Light source, provides the transmitted optical signal and determines capabilities of the system. For telecommunication purposes only lasers that are capable of being modulated at 20Mbit/s to 2.5Gb/s can meet current marketplace demands.

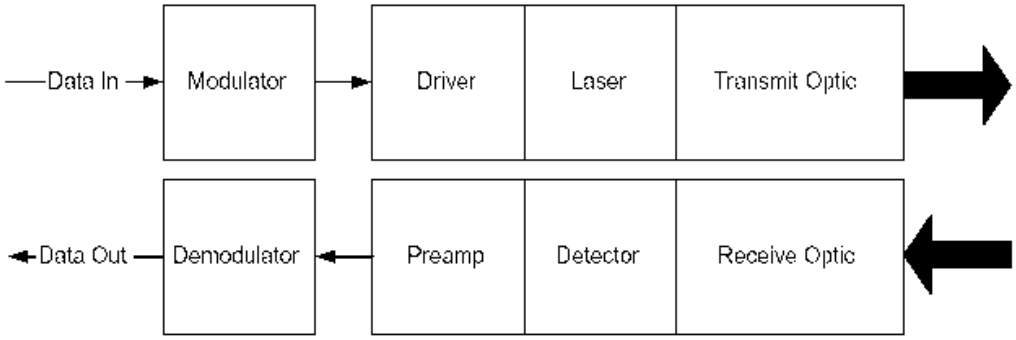

Figure 3.1. Free-space optics major subsystems

3.1.1 Transmitter

Free-space optical system transmitter designs are classified under two main titles; one is the transmitter electronics and the other is the optics.

3.1.1.1 Transmitter Electronics

Free-space optical communication transmitter systems are mainly based on idea of the electronic-to-optical conversion of data by means of integrated circuits, (drivers, modulators etc.) and laser. Although most of the commercial systems use electronic system some passive devices are on the marketplace to reduce overall cost.

In FSO the selection of light source dependent on the modulation scheme, output power and the applicable modulation speed. Lasers in the 780-925nm and 1525-1580nm spectral bands meet frequency requirements and are available off-the-shelf products. Although other operating wavelengths are used in commercial FSO systems, current trend is using 785nm, 850nm and 1550nm. Within these three wavelength windows FSO systems should have the following characteristics:

- Ability to operate at higher power levels (important for longer-distance FSO systems).
- High-speed modulation (important for high-speed FSO systems with internal modulation).
- Low power consumption (important for overall system design and maintenance).

- Ability to operate over a wide temperature range without major performance degradation (important for outdoor systems).
- Mean time between failure (MTBF) that exceeds 10yr.

To meet the above requirements, commercial FSO systems generally use VSCELs for shorter-IR wavelength range and Fabry-perot (FP) or distributed-feedback (DFB) lasers for operation in the longer-IR wavelength range. Most of the other types are not applicable for high-performance FSO systems.

VCSEL: VCSEL (780nm-850nm) lasers, which are increasingly applied in both fiber and FSO communication areas, have many attractive features. Invention of VSCELs diodes were a breakthrough in the transmission component market because of their exceptional cost and performance advantages over previously available technology. Most VSCELs have a reasonable, average power level of several miliwatts of output at high-speed operation and high reliability numbers for MTBF. The average power of the transmitter laser determines the link margin. Due to their low-cost ($30) in contrast to alternative lasers at the 780-850nm-wavelength range, VSCELs dominates the low-cost off –the-shelf systems, which are generally below 1Gbps. Because of their high efficiency, power dissipation is typically not an issue for VSCELs, and active cooling is not required. In addition, VSCELs emit light in the form of a circular shape instead of elliptical which is the case in most laser diodes. This round shape increases the coupling efficiency of the light beam into the fiber. The advance of VSCELs technology attracts much attention that many VCSEL manufacturers produce shorter-wavelength 780-850nm laser structures with direct modulation speeds beyond 2Gbps [9].

Fabry-Perot and Distributed-feedback Lasers: FP and DFB semiconductor lasers are designed firstly for maintaining high-speed communication purposes for fiber networks, which are operating at Gigabit speeds. FP and DFB lasers are based on InGaAs/InP semiconductor technology with operating wavelengths around 1550nm due to the low attenuation characteristics of optical fiber in this wavelength range. Today’s lower power 1550nm lasers have demonstrated excellent lifetime performance that satisfies the compulsory requirements of telecommunication industry. FSO technology applies these lasers for their low attenuation in 1550nm wavelength in clear air. DFB lasers can drive up to 40Gbit/s of modulation speeds under highly controlled conditions but they

are costly in comparison to FP lasers. Typical DFB laser operating at 2Gbps in about $785 whereas FP laser is around $150 [23].

Amplification Sources: Amplification source, such as EDFAs and semiconductor optical amplifiers (SOAs) are used to increase the power of lower-power laser sources. EDFA and SOA technologies can amplify both single and multiple closely spaced wavelengths simultaneously, which is Wavelength Division Multiplexing (WDM). EDFAs can drive the 1550nm optical output power of FSO system from few miliwatts to 1 and 2 W. At this time commercial EDFAs are quite expensive which limits the usage in FSO systems.

Modulators: FSO communication systems widely use intensity modulation direct detection (IM/DD) technique because of the complexity associated with phase and frequency modulation. In FSO communication two different modulation schemes are applied. One is the internal modulation of light where the diode lasers are driven with DC bias current to put the device above threshold then they are modulated with an AC current. AC current provides, for example, on-off keying (OOK) for data transmission, see Figure 3.2. The other modulation technique is the external modulation where the lasers are DC biased then the light passed through a modulator, see Figure 3.3.

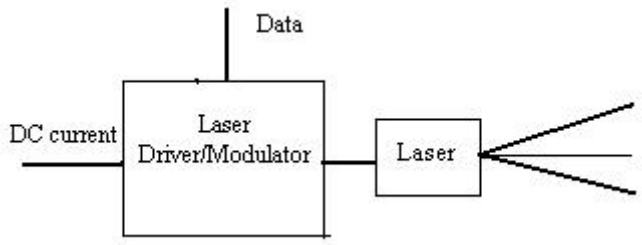

Figure 3.2. Internal Modulation

Internal modulation is widely applied in FSO systems due to the improvements in building integrated circuits, which supplies high-data rate modulation speeds (up to 40Gbps) with a considerable cost for lasers with low output powers. Although for higher power lasers, custom circuits or RF amplifiers are generally used, general acceptance on market is using low-power laser sources because of the cost considerations.

External modulation technique in contrast to internal modulation is based on the modulation of light beam as mentioned above. An external modulator restrains the light, functioning like an electrically activated shutter. As analog devices, external modulators allow the amount of light passed to vary from some maximum amount (P_{MAX}) to some minimum amount (P_{MIN}). P_{MIN} is the minimum light output from the external modulator, usually about 5% of the maximum value and P_{MAX} is the maximum light output from the external modulator, usually 3 to 5 dB less than the laser input. Most of the FSO systems are unlikely to use external modulators because of their high costs.

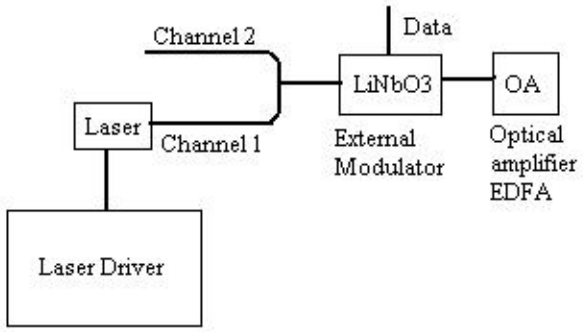

Figure 3.3. Shows an external modulation system applied in commercial Terralink 1000 FSO system where WDM is used at 1550nm wavelength.

Passive Transmitters: Passive systems, in other words all-optical FSO systems are designed to reduce the overall system cost by extracting the electro-optical conversion stages at both end, see Figure 3.4. Passive systems could be interpreted as a cut-in fiber technology where the light beam propagates through atmosphere between existing networks.

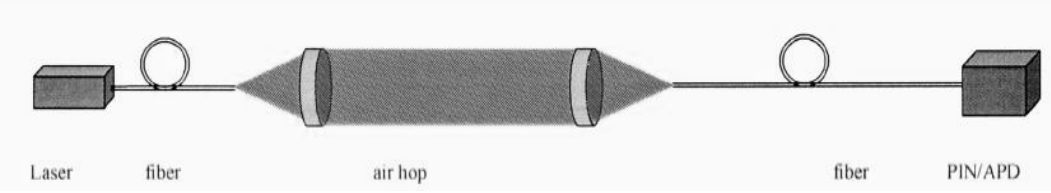

Figure 3.4. Principle of All-optical FSO systems

3.1.1.2 Transmitter Optics

FSO systems despite the different designs they all require some type of optical system to receive and transmit the optical signals. Typically, separate optical systems are used for transmitting and receiving functionality. In some minor cases same optical system is applied for both operations. In either cases, it is possible for the optical system to incorporate more than a-one aperture for either or both transmit and receive functions. There are several advantages to using a multiple-aperture in transmitter design, including greater resistance to complete blockage, better scintillation compensation, and inherent redundancy. However, in comparing systems, it is important to take into account the optical system aperture size inasmuch as a single large aperture and the total increase in the system cost.

An advantage of a multiple-aperture approach is that the potential for the temporary blockage of the beam by obstruction (e.g., birds) is significantly minimized since the probability that all beams would be blocked is drastically reduced. In addition, from operational perspective, using multiple apertures with multiple lasers on the transmitter can provide redundancy of the transmission path due to the laser source failure. Furthermore a multiple-aperture approach can be very beneficial in the reduction of scintillation.

A disadvantage of a multiple-aperture approach is that it increases system complexity because the light beam is coupled onto one or more receiver optics. Furthermore it is difficult to coalign transmit/receive aperture and maintain over a wide range temperature range. Figure 3.5 illustrates a commercial FSO system manufactured by Lighpointe where multiple transmit apertures are applied.

Transmitter Optic Design: The main purpose of the transmitter optic system is to produce a suitable beam divergence matching a desired beam diameter. Without transmitter optics the beam divergence angle of laser source would be very large, which is about 0.25-0.45 radian in semiconductor lasers. These angles lead to a beam diameter of 250m at a distance of 500m for 0.25 radian case respectively. In addition, a desired feature of the transmitter optics is that it should add a minimum of spherical aberrations because final spot size may be affected by these effects. Moreover, power-coupling efficiency is an important issue in FSO systems.

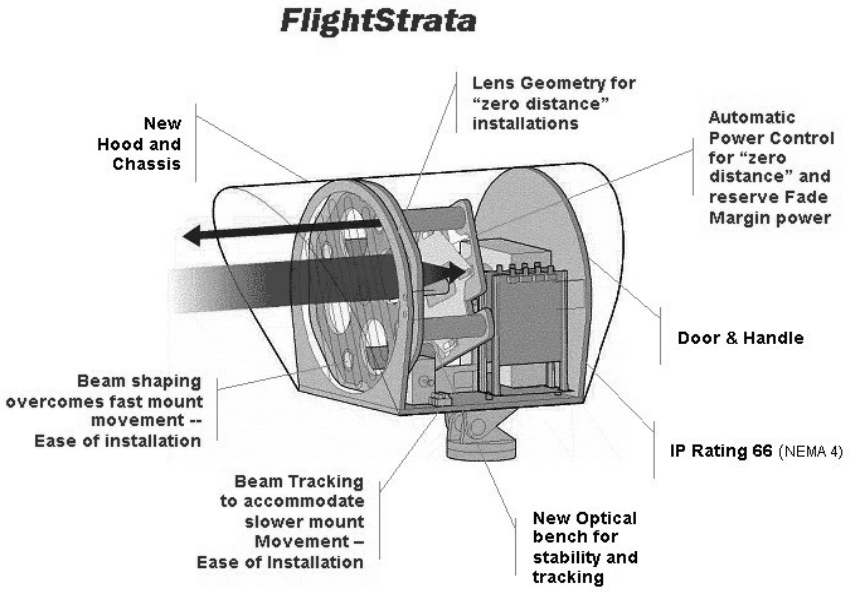

Figure 3.5. FlightStrata FSO transceiver manufactured by Lighpointe.

Transmitter optic systems are commonly designed by a single lens, which is perfectly situated close to the laser that collimates the outgoing laser beam. According to the propagation path length, receiver FOV and cost constraints several different lenses are applied in FSO systems. As an example both achromat lenses and plano-convex lenses with same diameters (20mm) achieves divergence angle of 1.3mrad according to the simulations in Zemax. Having the similar divergence angles achromat lenses introduce considerable difference in ray distribution. In achromat case the ray distribution is dense in the middle of the beam, and decrease towards the edges. Consequently, a relatively large fraction of the rays falls on the receiver aperture. The plano-convex singlet lens on the other hand does not exhibit the same behaviour with some of the power concentrated on the beam edges, see Figure 3.6.

An important observation regarding the beam divergence, the small diameter lenses having short focal lengths are adequate to launch power from the laser source. It is important to consider power losses even if the case of a few centimetres separation between the laser and the lens due to the high divergence angle of the laser sources (fiber-cable in passive systems). For a lens with f/# =2.54 located 6.45cm away from the laser diode with divergence angle of 0.29 radian theoretically introduces 3db power coupling loss without the Fresnel reflection loss.

Another observation regarding the power coupling is that the achromat lens as transmitter optics results in a small spot size because of the improved reduction in

spherical aberrations. On the other hand singlet lenses introduce large spot sizes, which are far beyond the diffraction-limited spot size.

Despite the numerous advantages of achromat lenses, they increase the system cost because of their high production expenses. Achromat lenses are basically made from two different lenses combined to reduce aberrations. Small spot sizes would not be the best solution to the FSO systems where the active tracking is not used. Excluding the passive FSO systems where fiber-to-fiber coupling is an issue and small spot sizes are required, spot size of FSO systems are depended on the active area of the receiver detector, FOV of receiver optic system and the displacement tolerance.

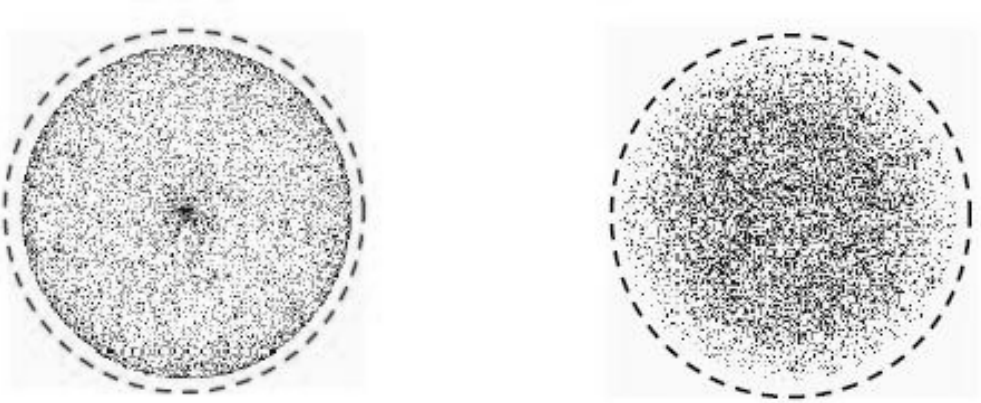

Figure 3.6. Pictures of the beam cross-sections. On the left plano-convex, on the right achromat lens.

3.1.2 Receiver

Receiver system including the both the electronics and the optics is the most challenging part of the FSO systems. Depending on the design intention (active, passive systems) receivers may be analysed under two separate sections, one is the receiver and the other is the electronics.

3.1.2.1 Receiver Optics

The design of the receiver optics is more crucial than the transmitter optics since it has to be accurately adjusted to the characteristics of the receiver detector. The receiver optics has the purpose of collecting as much as possible of incoming light beam

and couples it to the detector. One of the key challenges is maintaining transceiver alignment, which is defined as the allowable deviation from the optical axis.

Most important design solutions are divided in two categories:

- One-lens solutions, where the light is focused directly on the fiber detector using a single lens.
- Telescope based solutions, including both lens and mirror telescopes.

One-Lens Solutions: Since the main advantages of the FSO systems over competing wireless communications systems is the low-cost, today most of the vendors inclined to design single-lens solutions to achieve the lowest possible cost. Figure 3.7 shows a typical one-lens application in receiver. The main issue in receiver optics is to match the spot size to the detectors active area in order to avoid coupling losses. Otherwise the light incident on the detectors FOV will be lost.

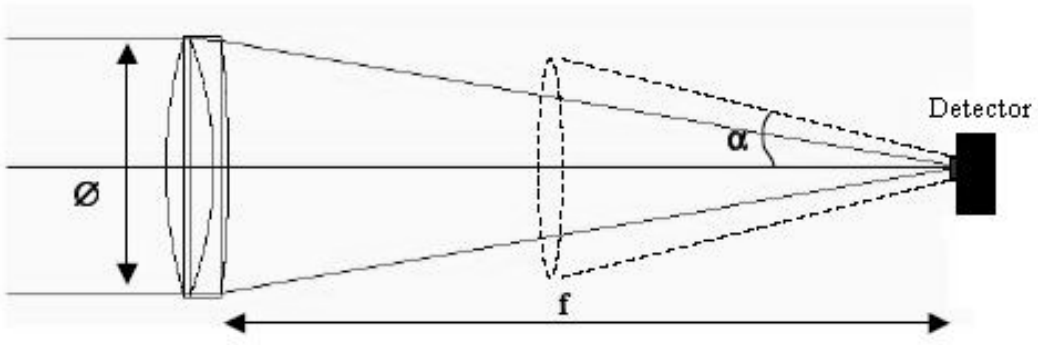

Figure 3.7. Principle of coupling light into the detector with a single lens.

The collected light beam by the receiver optic is designated by the aperture size of the receiver lens. As the aperture size increases f-number of lens, which is f/ϕ , decreases, which corresponds to a smaller spot size. The selection of lens then becomes a trade-off between the desired focal length and aperture size. Thus, a large aperture size in bulk optic implies generally a long focal length with a great increase in weight. In addition, spherical aberrations tend to increase with increased diameter.

Moreover, the price of bulk optics is much dependent on the lens diameter. For example, a 50mm lens from Melles Griot costs about $100 where the corresponding 82mm and 150mm lenses approximately $500 and $2000 respectively [15].

Telescope Solutions: Other main designs are based on telescopes. FSO system manufacturers build wide variety of telescopic solutions in system design. Some of the applied telescopes are Galilean telescope, Keplerian telescope and the Cassegrain mirror telescope.

- *Galilean telescope*: Figure 3.8 illustrates the principle scheme of Galilean telescope (light beam incident from right). A positive lens refracts the beam on a negative lens. The negative lens is placed at a distance equal to $f_2 + f_1$ from the positive lens. The diameter of the output beam depends on the focal lengths f_1, f_2. The magnification factor m, is given as [24]:

$$m = \frac{d_2}{d_1} = \frac{f_2}{f_1} \tag{3.1}$$

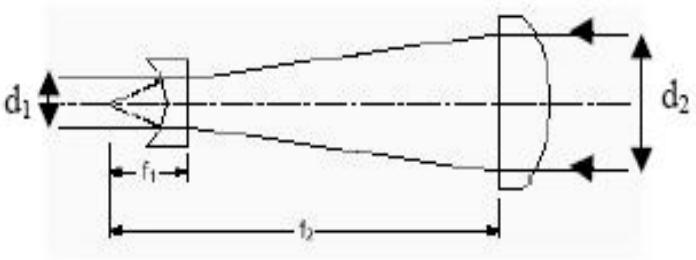

Figure 3.8. Principle of Galilean telescope

- *Keplerian telescope:* In figure 3.9 the principle of so-called Keplerian telescope is shown (light is incident from right) Two positive lenses, with different focal length and diameter, are used to reduce and collimate the beam. These lenses are placed apart a distance equal to $f_2 + f_1$ resulting in a collimated beam as output.

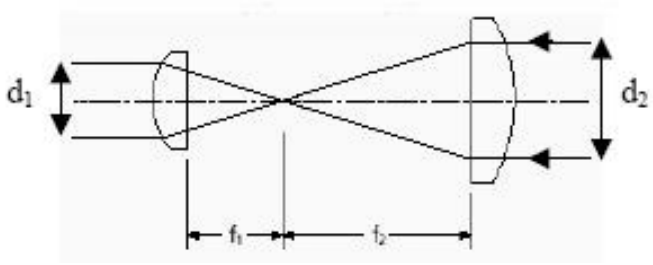

Figure 3.9. Principle of a Keplerian telescope

The magnification factor for Keplerian telescope is the same as for the Galilean telescope.

- *Cassegrain mirror telescope:* A mirror telescope can be designed to preserve diffraction-limited performance while retaining a large aperture. This feature introduces superior performance while FOV is limited mostly in case of passive systems (air-to-fiber coupling). The Cassegrain telescope is illustrated in figure 3.10. The incident rays hit a concave parabolic primary mirror and are reflected on a convex hyperbolic secondary mirror that forms the ultimate spot [25]. In comparison with a 50mm single lens a Cassegrain mirror telescope with 147mm primary mirror and 50mm secondary mirror which makes 50mm obscuration in the beam achieves seven times larger receiving area. Although their high efficiency Cassegrain telescopes need to be gold plated to obtain a sufficient surface and in addition their manufacturing process difficult and costly (127mm Cassegrain telescope costs more than $1000). Hence Cassegrain telescopes are not applied on low-cost commercial systems.

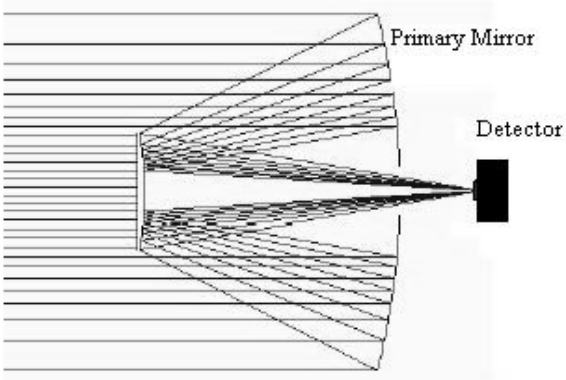

Figure 3.10. Principle of Cassegrain Mirror telescope

3.1.2.2 Receiver Optic System Design

Throughout previous section it is stated that the receiver optics is the most crucial part of the FSO system design. To balance the trade-off between the performance and cost is an important issue. Although their optimised achievements telescopic solutions introduce sharp rise in overall systems cost (Typical commercial 20Mbps FSO systems cost about $4000 where a Cassegrain mirror telescope adds an extra $1000). To overcome cost obstacle single off-the-shelf lens solutions are applied in investigated FSO system. In addition theorical calculations are carried out for comparison with the other receiver optics.

Light beam propagating through air to the receiver system spreads according to the divergence angle of the transmitter system. Received power as stated in equation 2.1.8 dependent on the aperture size of the lens. Figure 3.11 shows the corresponding received power for different aperture ranging from 1cm to 10cm where as the incoming beam differs in waist. It seen in the figure that as the aperture of the lens increases coupled power rises. However as mentioned in previous section there is a trade-off between the lens aperture and the focal lengths to achieve suitable spot-size.

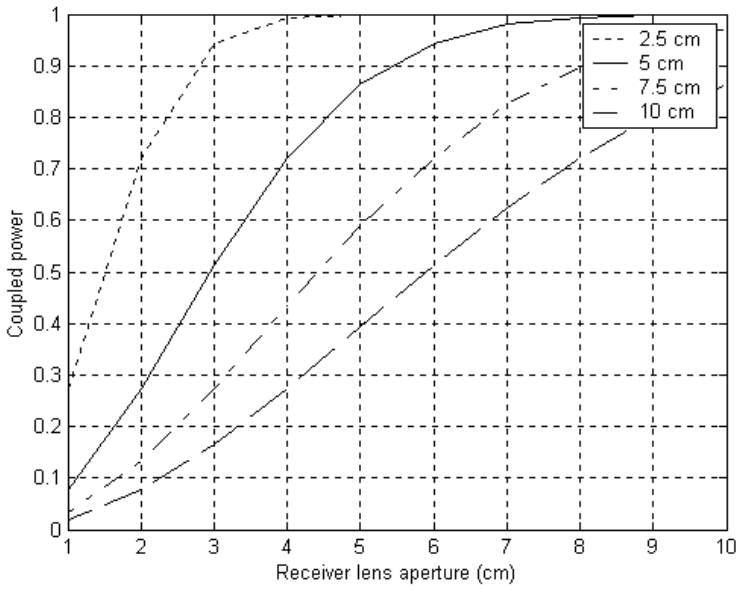

Figure 3.11. Coupled power change as the aperture and beam waist varies.

In addition to the coupled power considerations as stated in chapter 2 with the varying link distance and region FSO system is effected by the atmospheric events, which introduces deep fades to transmitted beam. Applying large receiver aperture or

multiple receiver apertures could considerably reduce scintillation. Figure 3.12 illustrates the probability of fading for FSO communication link as a function of threshold value for different receiver apertures (in the case of strong turbulence and the beam radius at the receiver lens aperture is 10cm).

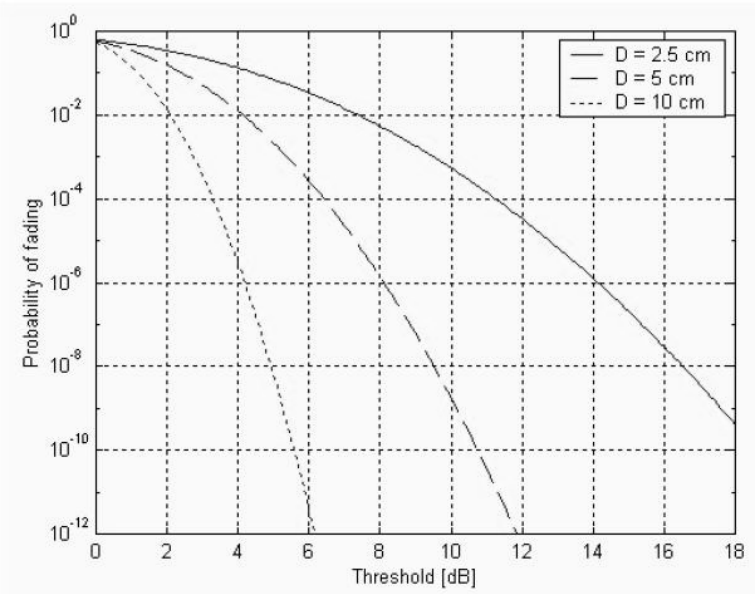

Figure 3.12. The probability of fading as a function of the threshold value F_t needed for different receiver apertures.

Both figure 3.11 and 3.12 shows that as the receiver lens aperture increases there is a considerable improvement in systems performance in means of fade margin and coupled power. However as the lens cost is geometrically related with the size, which prevents application of large aperture limits the maximum selectable lens aperture. In addition, bulk optic lens weight rises with the increasing aperture. Thus most commercial FSO systems use lens diameter about 50mm to 75mm.

Fresnel Lenses: As the bulk optic receiver systems aperture sizes are restricted with cost and weight considerations, alternative approaches are needed to be investigated. Apart from different bulk optic applications Fresnel lenses would be a solution to these constraints. Standard off-the-shelf 150mm Fresnel lens costs only $40 whereas bulk optic lenses costs more then $2000. In addition Fresnel lenses introduce considerable decrease in weight.

Invention of Fresnel lenses backs to 19th century after the recognition that the contour of the refracting surface of a conventional lens defines its focusing properties.

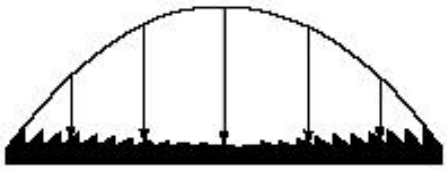

The bulk of material between the refracting surface has no effect (other than increasing absorption losses) on the optical properties of the lens. In Fresnel lens the bulk of material has been reduced by the extraction of a set of coaxial annular cylinders of material, as shown in Figure 3.13. Early Fresnel lenses are developed from glass which prevents high quality lens production and cost reduction. After improvements in computer and plastic technology Fresnel lenses reduced cost and improved in quality.

Figure 3.13. Construction of a Fresnel lens from its corresponding asphere. Each groove of the Fresnel lens is a small piece of the aspheric surface.

In addition, Fresnel lenses achieve superior improvement in aberrations resulting from the construction procedure. Spherical aberrations in general could be substantially reduced by aspheric surface lenses or doublet lenses (achromats). Since the Fresnel lenses are made from the beginning to correct aspheric profile, the notion of "correcting for spherical aberration" is not meaningful for Fresnel lenses. The combination of the aspheric surface (which eliminates longitudinal spherical aberration) and the thinness of the lens (which substantially reduces both absorption losses in the material and the change of those losses across the lens profile) allows Fresnel lenses with acceptable performance to be made with large apertures. Figure 3.14 shows correct application of

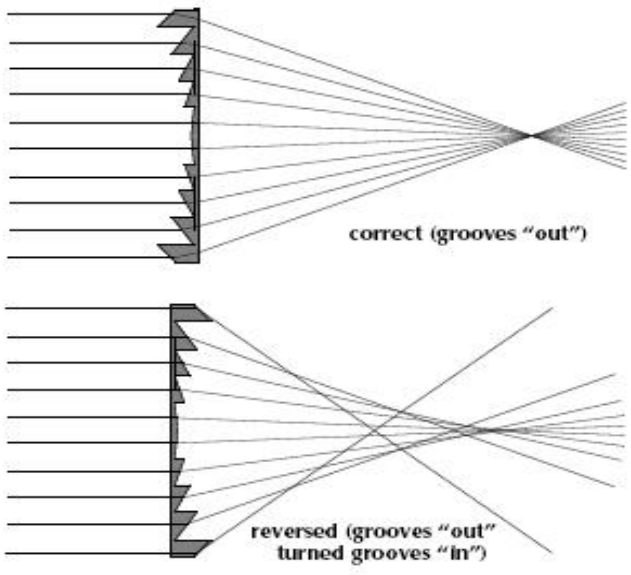

Fresnel lenses for aberration free application, incoming beam from left.

Figure 3.14. Fresnel lens, aberration free application.

Moreover, to apply Fresnel lens as the receiver optics in FSO communication systems, it is needed to verify their transmittance curve in interested operational wavelengths (785nm-1550nm) where the coupled power highly related to the lens efficiency. Dependent on the raw material applied in production process, relation between transmittance versus wavelength changes. Figure 3.15 shows typical Acrylic Fresnel lens transmittance as a function of wavelength obtained from Fresnel Technologies. Acrylic Fresnel lenses have a refractive index of 1.49 which similar to the bulk optic lenses. One other constraint is the Fresnel reflections according to the angle of incidence; see Figure 3.16 [26].

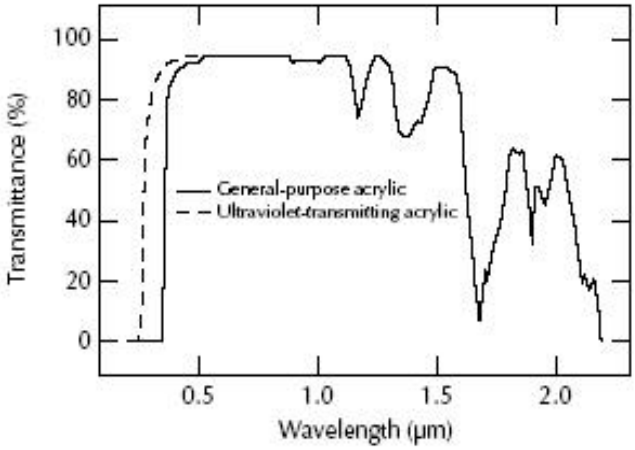

Figure 3.15. Transmittance of general-purpose acrylic and ultraviolet transmitting acrylic as a function of wavelength [26].

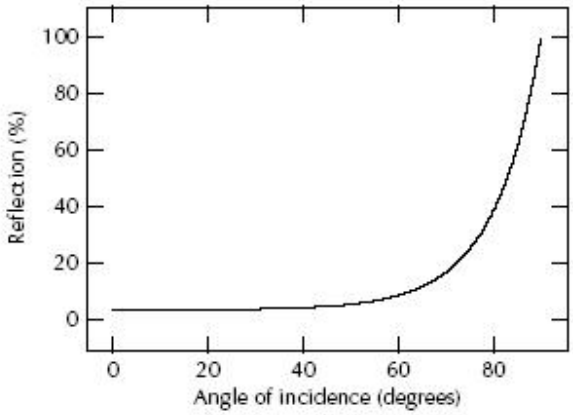

Figure 3.16. Loss due to reflection as a function of the angle of incidence. The angle shown is that between the incident ray and the nominal to the surface [26].

From equation 2.2.8 and under the assumption of incident ray and receiver lens on the same optical axes then the Fresnel reflections for the Acrylic Fresnel lens introduces R=0.039. Hence, Fresnel lens introduces 3.9 % power loss where single bulk optic lens losses 4 % of incident power for every glass-air interface.

Thus, Fresnel lens is could be a viable solution to the existing low-cost FSO communication systems. Throughout the experimental calculations performance comparison between bulk optic lens with a diameter of 50mm and Fresnel with D=127mm off-the-shelf lenses are applied.

3.1.2.3 Detectors

Making comparison between transmitter and receiver electronics receiver side has very tight constraints. The two of the most common detector material systems used in the near-IR spectral range are based on SI or Indium Gallium arsenide (InGaAs) technology. Although Germanium covers the operating wavelength range of commercial FSO systems, they are not applied due to their high dark current values. All these materials are not tuned to a specific wavelength, which enlarges the application range but in addition limits the detection of single wavelengths. For example, when WDM technique is realised in FSO then wavelength filters must be incorporated into the design.

Short-wavelength detectors: Silicon (Si) is the most commonly used detector material in the visible and near IR wavelength range. Si technology is fairly developed from the invention and gain ability to detect low levels of light. Si has a wavelength-dependent spectral response, which needed to match to the operation wavelength of the transmitter. Typical Si detectors have a spectral response maximum sensitivity around 780-850nm, making these detectors ideal for combined application with short-wavelength VCSELs. On the other hand Si sensitivity drops off dramatically for wavelengths beyond 1μm. Thus this wavelength is the cut-off for the Si detectors. In addition Si detectors can operate at very high frequencies, a recent commercial 850nm systems applied 10Gbps to market.

Lower-bandwidth (1 Gbps) Si PIN and Si APD detectors are widely available. Si-PIN detectors commonly integrated with pre-amplifiers. In these detectors, sensitivity is a function of signal modulation bandwidth, which decreases as the detection bandwidth increases. Typical sensitivity values for Si-PIN diode around –34dBm at 155Mbps. Si-APDs are more sensitive in contrast to Si-PIN diodes resulting from internal amplification (avalanche) process. Therefore, Si-APD detectors are higly useful for detection in FSO systems. Sensitivity values for higher-bandwidth applications can be as low as –55dBm at speeds of several Mbps (-46dBm at 622Mbps). Si detectors are quite large in size while maintaining high communication speeds. This feature minimises losses when the light is focused on the detector with either large-diameter lens or telescopes used.

Long-Wavelength Detectors: InGaAs is the most commonly used detector material for the longer wavelength range. Similar to Si, InGaAs spectral response depends on the detection wavelength. As the spectral response of InGaAs detectors are optimised between 1300-1550nm. As a result nearly all of the longer wavelength fiber-optic systems use InGaAs detectors. Because of the drastic decrease in sensitivity toward the shorter wavelength range, InGaAs detectors are typically not used in the 780-850nm-wavelength range.

The primary benefit of InGaAs detectors is their extremely high bandwidth capability when combined with APD technology. Sensitivity values for higher-bandwidth applications are as low as –46dBm at 155Mbps. However InGaAs detectors when operating at higher speeds are smaller in size than their Si counterparts. This decreases the displacement tolerance of FSO system while coupling incident light.

Table 3.1 presents some of the more common detector materials applied in FSO systems and their basic properties.

Table 3.1. Selected detector material systems and basic properties.

Material/Structure	Wavelength (nm)	Responsivity (A/W)	Gain
Silicon PIN	300 – 1100	0.5	1
Germanium PIN	500 – 1800	0.7	1
InGaAs PIN	1000 – 1700	0.9	1
Silicon APD	400 – 1000	77	150
Germanium APD	800 – 1300	7	10
InGaAs APD	1000 – 1700	9	10

3.2 Laser Safety

In FSO technology as the propagation medium is air, safety concern is an important issue. High-power laser beams possibly cause injury to skin, but the primary safety problem is the potential exposure of the eye to the beam. Eye focuses the incident laser light to a point on the retina depending upon wavelength. The specific wavelength is important because only certain wavelengths – between approximately 0.4 and 1.4μm – are focused by the eye onto the retina. Other wavelengths tend to be absorbed by the front part of the eye (cornea) before the energy is focused and concentrated. The absorption of the eye varies with wavelength, see Figure 3.17. The absorption of the cornea is much higher for the wavelengths longer than 1.4μm in comparison to the shorter wavelengths. In addition to the absorption coefficient, eye has another natural response, which is reflexion that is turning away from a bright visible light. However wavelengths longer than 0.7μm do not trigger a reflexion response, because they are invisible. According to the ANSI standard limits for eye safety (for a 10-second exposure) are 100mW/cm^2 for 1550nm and 1.5mW/cm^2 for 785nm [27].

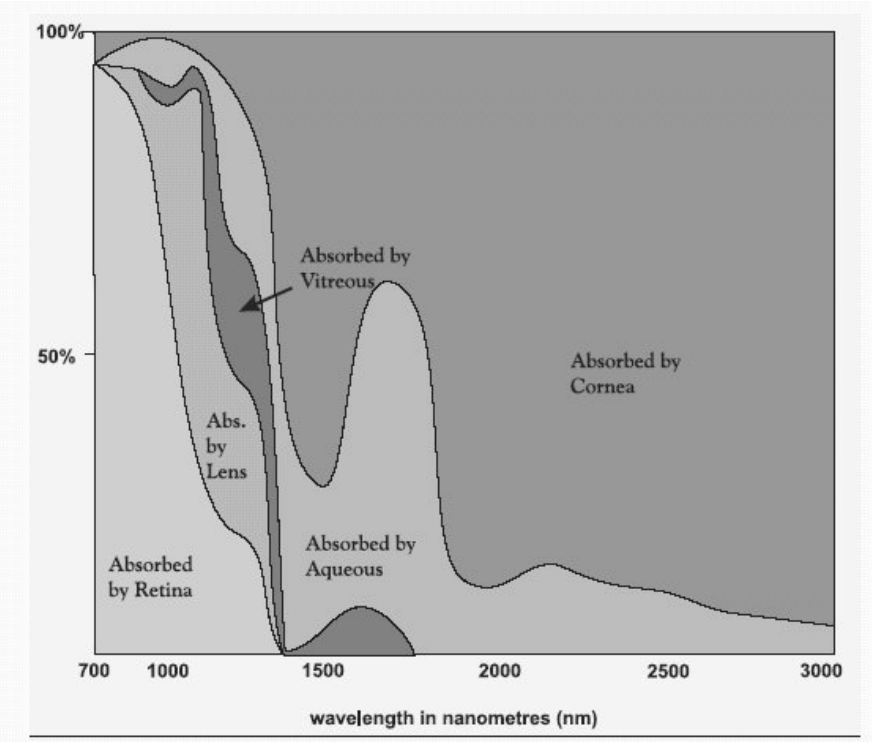

Figure 3.17. Absorption of infrared radiation as a function of wavelength.

Chapter 4

LINK BUDGET AND DISPLACEMENT ANALYSIS

Throughout the preceding chapters theoretical overview and link design schemes of free-space optical communication systems are examined including the alternative optical receiver for mitigating severe weather conditions. This chapter focuses on the theorical comparison of bulk optic FSO systems having the Fresnel optic unit under varying atmospheric conditions and displacement analysis of 785nm and 1500nm systems.

4.1 System Overview

In order to analyse the effects of atmospheric events over the FSO system, experimental communication link is established at the campus of Izmir Institute of Technology between two buildings. Figure 4.1 illustrates the communication link where both the transmitter and receiver devices are installed at the electro-optic laboratory in order to make the design simpler. To couple the transmitted beam from the transmitter to the receiver a mirror is placed at the classroom building which has high reflection coefficient. Overall propagation path is approximately 35metre where both transmitter and receiver assemblies are behind the laboratory windows.

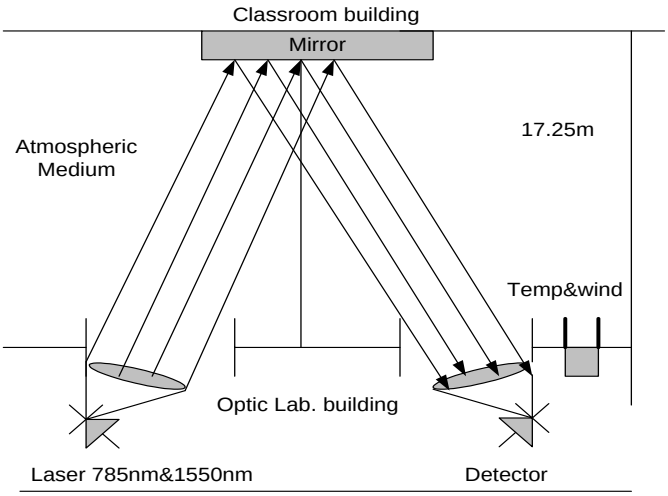

Figure 4.1. Transmission system over 35m range.

At the receiver end both bulk optic and Fresnel optic single lenses are applied for beam coupling to the detector at two different wavelengths 785nm and 1550nm.

As mentioned previously FSO systems are severely affected by the atmospheric events. To observe the performance of both proposed Fresnel optic and the bulk optic system under varying atmospheric conditions communication link is designed to acquire the receiver power of both continuous and the digital transmitted signals. Table 4.1 lists the equipments used in the experimental link design.

Table 4.1 Equipments

Transmitter assembly:	Mobile breadbroad assembled on rails with lens holder.
Lens assembly:	Adjustable lens holders assembled on carriers centred on rails.
Alignment laser:	Newport 1.5mW He-Ne laser, peak wavelength 633nm.
Lasers:	785nm 70mW Sanyo DL7140 single mode index guide structure semiconductor laser. 1550nm 5mW Mitsubishi ML976H6F InGaAsP Single transverse mode Fabry-Perot semiconductor laser.
Lens:	Newport KBX055 bi-convex lens with *f=6.45cm, D=2.54cm*. Newport KPX187 plano-convex lens *f=10cm, D=5.0cm.* Fresnel Technologies Fresnel lens *f=25.4cm, D=12.7cm.*
Detectors:	Newport 813-BB-21 Silicon detector, operation range 300nm-1100nm, Rise/Fall time <300ps. Assembled on x-y-z microblock. Newport 818-BB-31 InGaAs detector, operation range 1000-1600nm, Rise/Fall time < 200ps. Assembled on x-y-z microblock.
Power Meter:	Newport 818-2S-I InGaAs/Si Universal fiber optic detector, operation range 400-1650nm.
Laser Driver:	Thorlabs IP500 500mA laser diode driver, constant current or constant power operation mode.

4.2 Link Analysis

As stated in chapter two, laser light out of a laser diode could be represented by Gaussian beam approximation, which is a solution to Helmholtz equations. Throughout the proceeding calculations laser light is assumed to behave as Gaussian beam. Figure 4.2 shows the simplified model of established FSO system in place of Figure 4.1 for the link budget calculations.

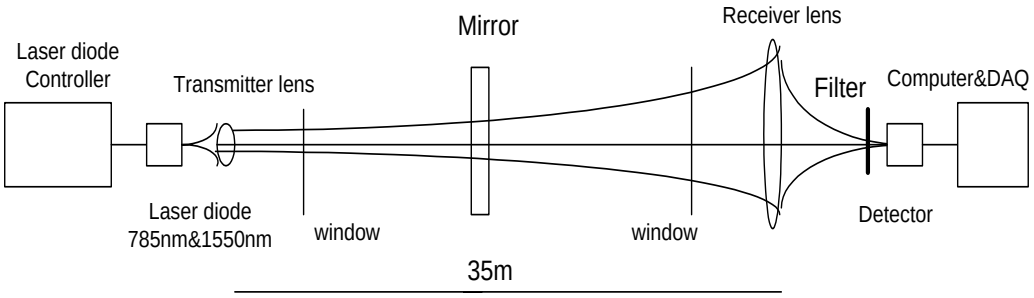

Figure 4.2. Simple model of FSO communication link between laboratory building and the classroom building.

Gaussion Beam Transmission through Single Lens: As seen from the figure 4.2 transmitter laser is placed a few centimetres apart from the semiconductor laser to achieve minimum divergence angle. Figure 4.3 illustrates the propagation of Gaussian beam through a thin lens.

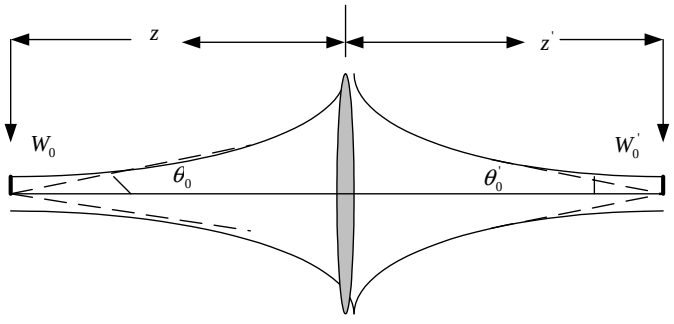

Figure 4.3. Transmission through thin lens.

Transmission equalities are defined as follows [11]:

Waist radius $w_0^{'} = Mw_0$ (4.2.1)

Waist location $(z' - f) = M^2 (z - f)$ (4.2.2)

Divergence $\theta_0' = \frac{\theta_0}{M}$ (4.2.3)

Where M is defined as $M = \left| \frac{f}{z - f} \right|$.

4.2.1 Link Analysis for 785nm Wavelength

Sanyo 785nm-laser diode applied in the experimental link has the following properties:

Divergence angle: $\theta_0 = 12^o = 0.21 rad$

Beam waist: $w_0 = 1.19 \mu m$

Rayleigh distance: $z_0 = 5.66 \mu m$

Output power: $p_0 = 70 mW (18.45 dBm)$

Although the typical output of the semiconductor laser is 70mW the measured output power of the laser at the laser diode aperture is 73mW (18.63dBm). In order to achieve small divergence angle laser is placed close to the focal point (f=6.45cm) of the transmitter lens. Due to the unguided beam propagation through the lens some of the transmitted power is useless. To ratio of the power coupled to the lens, given by the equation 2.1.8, is dependent to the circle of radius (ρ_0) of the lens and the beam waist. Power coupled at the distance 6.42cm apart from the laser is 17.83dBm (0.8dBm coupling loss). Fresnel reflections at the lens add (equation 2.2.8) extra 0.37dB power loss, which reduces the power to 17.46dBm. Furthermore laboratory windows also introduce Fresnel reflections (0.75dB loss), and then the total power is decreased to 16.71dBm.

Transmitter lens alters the beam waist, waist location and the divergence angle of the beam. From the equations 4.2.1 to 4.2.3:

M=215, $\theta_0' = 0.976 mrad$, $w_0' = 255.8 \mu m$. Waist location is $z' = 13.8 m$.

Beam waist at 17.5m distance from equation 2.1.9 is $w'(z) = 0.36 cm$. Laser beam propagating through aperture (in this case mirror) maintains its Gaussian nature when the truncation ratio is smaller then 0.5 [28]. Equation 2.2.5 defines the truncation

ratio where *T=0.14* is this case (mirror diameter is 2.5cm) then in this link laser beam is also Gaussian after the lens.

Atmospheric transmission medium introduces attenuation to the communication link as stated in chapter two. From the equations 2.3.7 and 2.3.12 with three different conditions weather introduces loss of 0.01dB in clear air, 0.06dBm in haze and 0.75dBm in fog (17.5m link distance).

Power coupled to the mirror is nearly 100% from the calculation 2.1.8 due the small beam waist and coupling efficiency of mirror that restricts the Fresnel reflections.

At the receiver end, the laboratory windows add 0.75dB power loss like the windows at the transmitter side. Overall system power loss from lens to lens according to the theoretical calculations varies from 2.9dB to 4.4dB.

The coupled power to the lens at the receiver depends on the receiver aperture size and the beam waist *w (z)*. Beam waist at the receiver end from the equation 2.1.9 calculated as 2cm. Table 4.2 shows the power coupled to the receiver lens.

Table 4.2. Power collected by the receiver lens (35m).

Link range 35m	Clear air	Haze	Fog
Normal lens D=5cm	15.37dBm	15.27dBm	13.9dBm
Fresnel lens: D=12.7cm	15.56dBm	15.46dBm	14.08dBm

Spot Size: The spot size of the bulk optic receiver lens is calculated from the equations 2.2.7 and 2.2.4 where *d=0.97mm* due to the spherical aberrations and $d=3.09\,\mu m$ for K=2 (uniform illumination assumptions) due to the diffraction-limited solutions. Spot size of the Fresnel lens is *d=2.13mm* and $d=3.14\ \mu m$ respectively. Lenses used in this project are not diffraction-limited so spot size due to the spherical aberrations dominates the overall spot.

The Coupled Power to the Detector: Receiver detector is placed 16cm away from the lens to raise the displacement tolerance of the receiver system. In addition a line filter and an attenuator (%10 transmittance) are mounted in front of the active area of the detector for decreasing the sun light effects (Line filter has 45% coupling efficiency) and the high received power. Figure 4.4 and figure 4.5 shows the detailed receiver scheme of the experimental FSO link.

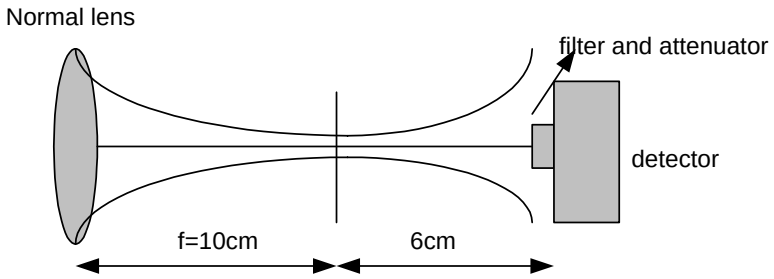

Figure 4.4. Receiver scheme (normal lens).

Beam waist at the detector end of the receiver (for normal lens) is $w''(z) = 1.2cm$, see figure 4.4. Active area of the detector 813-BB-21 is $0.12\,mm^2$. Power received at the detector defined by the equation 2.1.9 while $\rho_0 = 0.19mm$ where the coupled power is $P_{coupled} = 0.77\mu W(-31.13dBm)$.

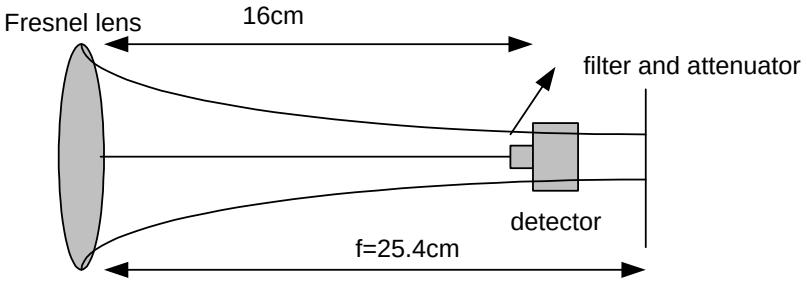

Figure 4.5. Receiver scheme (Fresnel lens).

Beam waist in the case of Fresnel lens is $w_f''(z) = 0.752cm$, see figure 4.5. Similar to the normal lens calculation power at the detector is defined by equation 2.1.9 where $P_{coupled} = 2\mu W(-27dBm)$.

Displacement Calculation: As stated in chapter two, alignment tolerance is defined by F.O.V which is calculated by the equation 2.2.9. r_s is the tolerable beam centre displacement. Receiver detector couples incoming power according to the radius of active area *(0.19mm).* For the normal lens case with the assumption of 3dB loss resulting from the beam centre deviation is $r_s = 0.095mm$. F.O.V is $2\alpha = 1.9mrad$. For the Fresnel lens r_s is different from the normal lens due to the focal length and high power coupling efficiency in contrast to the normal lens. For $r_s = 0.475mm$ F.O.V is

2α=3.74mrad. It is seen that as the receiver aperture size increases the F.O.V increases too. In experimental link realisation Fresnel lens with high focal length is applied, which introduces a considerable loss to the F.O.V. Thus, for high coupling efficiency and FOV tolerances the receiver aperture having short focal length and large aperture size should be applied.

4.2.2 Link analysis for 1550nm Wavelength

Similar to the 785nm-laser the 1550nm-laser link is established between the two buildings described in previous sections. Fabry-Perot 1550nm-laser diode has the following properties:

Divergence angle: $\theta_0 = 25^o = 0.436rad$

Beam waist: $w_0 = 1.13\mu m$

Rayleigh range: $z_0 = 2.59\mu m$

Output power: $p_0 = 5mW(7dBm)$.

To find out the output power of the laser at the aperture beam profile of 1550nm laser is measured. Unlike the typical operation value from the specifications the output power is measured as *P=4.84mW (6.84dBm).* In order to achieve small divergence angle the laser is placed as close as to the focal point (f=6.45cm) of the transmitter lens. The ratio of the power coupled to the lens, given by the equation 2.1.8, is dependent to the circle of radius (ρ_0) of the lens and the beam waist. Power coupled at the distance 6.43cm apart from the laser is 2.12dBm (4.72dB coupling loss). Fresnel reflections at the lens add (equation 2.2.8) extra 0.37dB-power loss, which reduces the power to 1.75dBm. Furthermore laboratory windows also introduce Fresnel reflections (0.75dB loss) then the total power is decreased to 1dBm.

Divergence angle and waist location of the beam can be calculated from the equations 4.2.1 to 4.2.3:

M=322.5, $\theta_0^{'} = 1.35mrad$, $w_0^{'} = 364.4\mu m$. Waist location is $z^{'} = 20.73m$.

Beam waist at 17.5m distant from equation 2.1.9 is $w^{'}(z) = 0.43cm$. Then the truncation ratio at the mirror *T=0.17* is this case (mirror diameter is 2.5cm) then the laser beam similar to the 785nm laser is also Gaussian.

Propagation through atmospheric medium introduces a wavelength dependent attenuation resulted with a difference between 1550nm link and 785nm link. From the equation 2.3.7 the different weather conditions introduces loss of 0.006dB in clear air, 0.055dBm in haze and 0.735dBm in fog (17.5m link distance).

Overall system introduces loss of 7dB up to 7.7dB dependent on the atmospheric conditions. Table 4.3 shows the overall system analysis after propagation between two buildings:

Table 4.3. Power collected by the receiver lens (1550nm, 35m).

Link Range 35m	Clear air	Haze	Fog
Normal lens D=5cm	-0.276dBm	-0.325dBm	-1dBm
Fresnel lens: D=12.7cm	-0.126dBm	-0.175dBm	-0.855dBm

Spot Size: The Spot size of the receiver lens is calculated as *d=0.97mm* and for diffraction-limited case $d=6.07\,\mu m$ when K=2 (uniform illumination assumptions). For Fresnel lens *d=2.13mm* and $d=6.2\,\mu m$ respectively. The spot size is larger at 1550nm then the 785nm case.

Coupled Power to the Detector: Similar to the 785nm link at 1550nm wavelength, receiver lens is placed at the minimum waist point of the laser to couple the maximum power to the detector. In contrast to the 785nm laser power is considerably low which prevents saturation of the detector. Line filter is placed between detector and lens to reduce the atmospheric noise (%50 transmission efficiency). Figure 4.6 illustrates the receiver scheme.

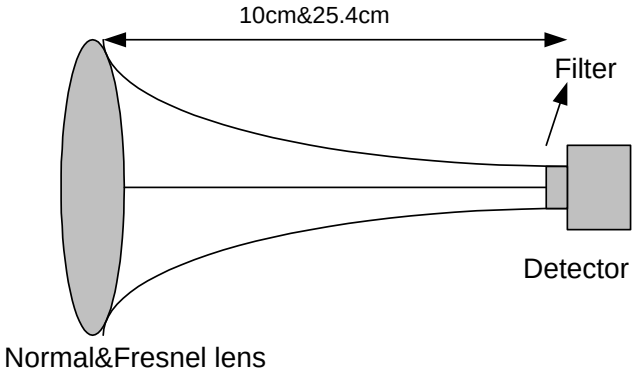

Figure 4.6. Receiver scheme 1550nm-laser link.

Beam waist at the detector end of the receiver (for normal lens) is equal to the half-spot size which is $w''(z) = 0.97mm$, see figure 4.6. Active area of the detector 813-BB-31 is $7.9\times10^{-3}\ mm^2$. Power collected at the detector is defined by the equation 2.1.9 while $\rho_0 = 0.05mm$ where coupled power is $P_{coupled} = 2.49\mu W(-26dBm)$. Beam waist in the case of Fresnel lens is $w_f''(z) = 2.13mm$, see figure 4.6. Similar to the normal lens calculation power at the detector defined by equation 2.1.9 where $P_{coupled} = 0.27\mu W(-35.68dBm)$. Unlike the 785nm case in the 1550nm wavelength the power coupled in Fresnel lens is less than the normal lens. This dilemma is resulted due to the high focal length of the Fresnel lens. To achieve the smallest possible spot size low f-number lenses are suggested in FSO systems.

Displacement Calculation: At 1550nm wavelength r_s is *0.025mm* for the normal lens case with the assumption of 3dB loss resulting from the beam centre deviation. F.O.V is 2α*=0.5mrad.* For the Fresnel lens r_s is different from the normal lens due to the focal length and high power coupling efficiency in contrast to normal lens; r_s =0.125*mm.* F.O.V is 2α*=1mrad.* It is seen that when the receiver aperture size increases the F.O.V increases. As stated in 785nm link for high coupling efficiency and large F.O.V tolerances the receiver aperture with short focal length and large aperture size selection would be applied.

Throughout the calculation for the 785nm and the 1550nm it is seen that the displacement tolerance and power coupling efficiency are highly related to the receiver lens aperture and the detectors active area. As the aperture size and active area increases the overall system performance increases. Thus, large aperture lenses with low f-number are applied in FSO systems. However as mentioned in previous chapters that the bulk optic lens cost rises with the increase in the aperture size. Hence, Fresnel lenses could be a feasible solution according to the calculation in this chapter.

.

Chapter 5

RESULTS AND CONCLUSION

The main objective of this chapter is the experimental investigation of FSO laser link performance, which is established between two buildings at engineering faculty. Comparison with the theoretical model developed in the previous chapter will also be carried out in this chapter. So that the performances of Fresnel and bulk optic receiver systems will be compared in terms of displacement tolerances, power coupling efficiency and spot size at two different laser wavelengths (785nm and 1550nm).

As a first step laboratory tests are performed in order to compare the intensity distribution of both the bulk optic and the Fresnel optic lenses. The purpose of testing these lenses in laboratory is to find out the coupling efficiency differences between two optical systems. These two tests are performed at two different distances, 7.15m and 68m –in the laboratory-.

Secondly field tests are performed under varying atmospheric conditions between two buildings, see Figure 4.1. In field tests two different lasers operating at 785nm and 1550nm are used to observe the intensity fluctuation due to the varying atmospheric conditions such as temperature and wind.

5.1 Laboratory Tests: Distance 7.15m and 68m

Figure 5.1 illustrates the simplified model of the experimental laser link established between the laboratories. During the tests both the 785nm and 1550nm lasers are applied at two different distances 7.15m and 68m. For the system alignment

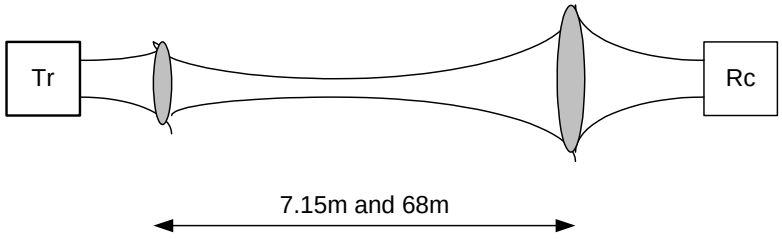

Figure 5.1. Laboratory laser link set-up.

visible 633nm He-Ne laser is used. In the experiments Newport D=2.54cm bi-convex lens used as the transmitter lens and at the receiver side Newport D=5.08cm plano-convex and Fresnel Technologies D=12.7cm Fresnel lens are deployed as the receiver lenses. For comparison purposes the incident beam waist at the receiver end of the system is approximately set to 5cm for both 7.15m and 68m. Figure 5.2 and 5.3 shows the intensity distribution at the receiver detector for the 1550nm-laser (Newport 818-2S-I).

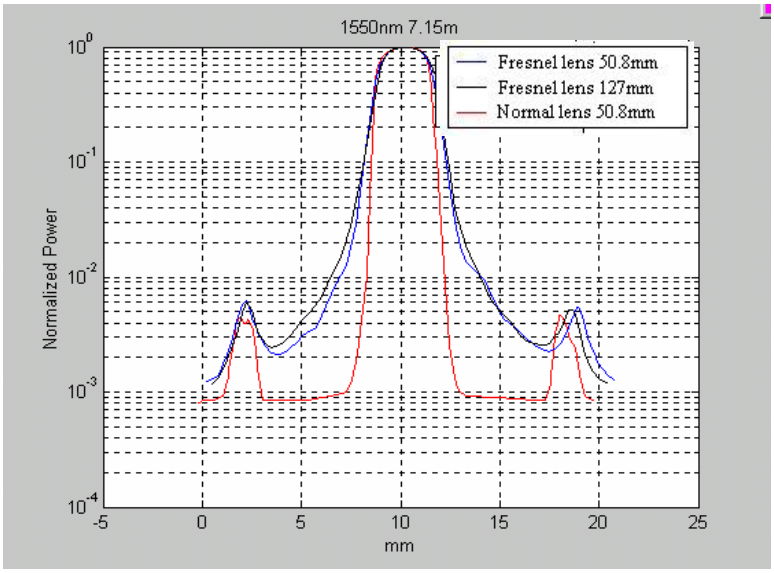

Figure 5.2. Intensity distribution of laser beam at 1550nm at 7.15m distance for the three different lenses.

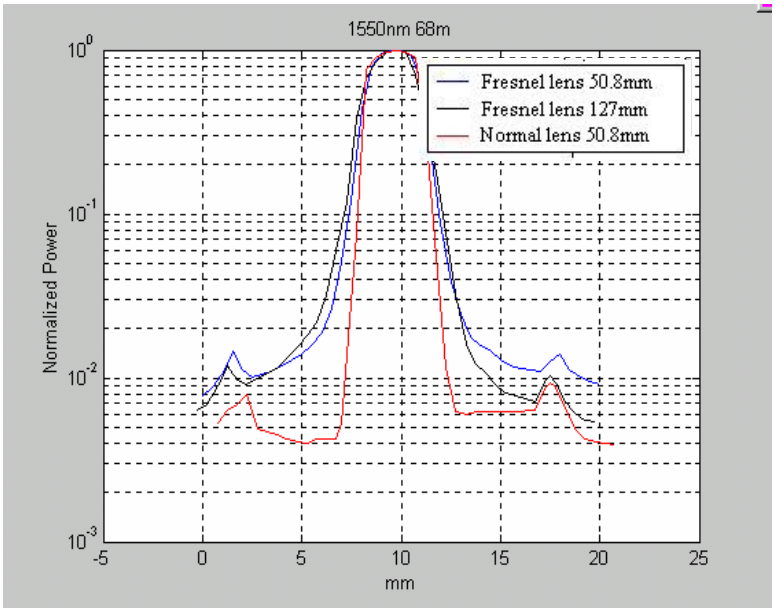

Figure 5.3. Intensity distribution of laser beam at 1550nm at 68m for the three different lenses.

Table 5.1 gives the results of spot size, collected power and displacement tolerances of both lenses measured from Figure 5.2 and 5.3.

Table 5.1. Displacement tolerance, spot size and received power for 7.15m and 68m.

Receiver 7.15m/68m (1550nm)	r_s	Power (dBm)	Spot size
Normal lens	1.38mm	-1.5dBm	3.23mm
Fresnel lens (D=5cm)	1.47mm	-2.59dBm	3.92mm
Fresnel lens (D=12.7cm)	1.47mm	-2.35dBm	4.04mm
Normal lens	1.42mm	-13.28dBm	3.6mm
Fresnel lens (D=5cm)	1.52mm	-13.47dBm	4.25mm
Fresnel lens (D=12.7cm)	1.5mm	-11.55dBm	4.6mm

Experimental results show that the Fresnel lenses in contrast to bulk optic lenses introduces larger spot sizes. Larger spot size results in decrease with a loss in the power coupling efficiency. For the 7.15m case in Table 5.1 Fresnel lens approximately couples 1dB less than the bulk optic lens. From the Figures 5.2 and 5.3 it is seen that the Fresnel lens intensity distribution is wider at the edges, which is resulted with larger displacement tolerance values. (r_s values calculated for 3dB power loss).

Similar to the 1550nm-laser Figure 5.4 and 5.5 show the intensity distribution for the 785nm-laser.

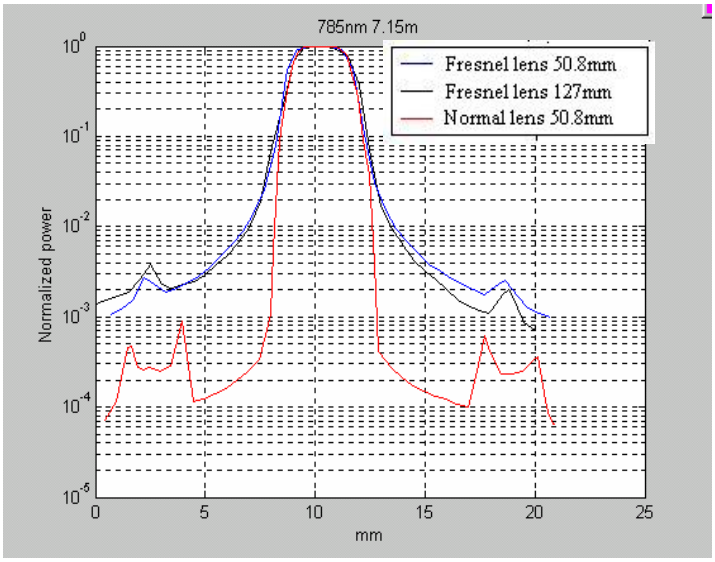

Figure 5.4. Intensity distribution of laser beam at 785nm at the 7.15m distance for the three different lenses.

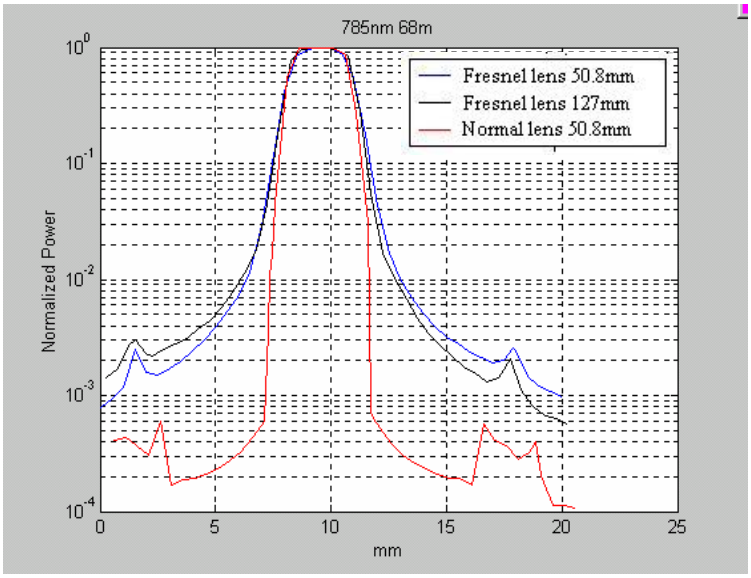

Figure 5.5. Intensity distribution of laser beam at 785nm at 68m distance for different lenses.

Table 5.2 gives the results of spot size, collected power, received power and displacement tolerances of both lenses are calculated from Figure 5.4 and 5.5.

Table 5.2. Displacement tolerance, spot size and received power for 7.15m and 68m.

Receiver 7.15m/68m (785nm)	r_s	Power (dBm)	Spot size
Normal lens	1.39mm	14.62dBm	3.6mm
Fresnel lens (D=5cm)	1.52mm	13.65dBm	3.81mm
Fresnel lens (D=12.7cm)	1.45mm	13.73dBm	3.98mm
Normal lens	1.38mm	11dBm	3.46mm
Fresnel lens (D=5cm)	1.46mm	10.24dBm	4.05mm
Fresnel lens (D=12.7cm)	1.45mm	11.37dBm	4.2mm

Similar to the 1550nm-laser link case in the 785nm-laser link Fresnel lens spot size is larger then the bulk optic lens which reduces the coupled power to the detector approximately 1dB. On the other hand displacement tolerance for the Fresnel lens is larger than bulk optic lens, which also resembles to the 1550nm measurements.

Thus, the laboratory tests show that the performance of Fresnel lenses is slightly less than the bulk optic lenses. However, due to the high displacement tolerances and low prices Fresnel lenses could be alternative solutions to the existing FSO links.

5.2 Free-Space Link in Atmospheric Condition

After performing indoor tests in the laboratory the system is established between two buildings of the Engineering Faculty to collect data of the intensity through the link and atmospheric parameters; wind and temperature. Since the transmitter and the receiver units are placed at the same laboratory (opto-electronic Lab.) a mirror is fixed on the wall of the classroom building to reflect the light beam back to the receiver unit. Total distance that the light beam travels is 63 meters. The system performance is evaluated at two different wavelengths, 785 nm and 1550 nm. However, two systems, 785nm and 1550nm, can not be run at the same time because the laser driver unit is designed for driving a single laser at a time. The data for the wind, the temperature and the intensity of the systems having various configurations have been collected for a period of 24 hours. The systems that will be presented below are designed to use single lens receiver and single lens transmitter optical units. Also, the line filters at 785 nm and 1550 nm are installed in front of the detector in order to eliminate the ambient light fluctuations due to daylight. Neutral density filter as an attenuator is also used when it is needed to adjust the dynamic ranges of the input intensity to the detector.

5.2.1 785nm-Laser Link Field Tests

The 785nm-laser link has been observed from 29th of June till third of July 2004. Experimental link scheme as defined in previous chapter consists of 70mW laser diode at the transmitter side with the bi-convex D=2.54cm lens as the collimator lens and both normal and Fresnel lens (diameter of 12.7cm and 5.08cm) as the receiver aperture for coupling the incident laser beam to the receiver. During the link installations He-Ne laser is used for link alignment purposes. At the receiver side as stated in chapter four 785nm line-filter and an attenuator (-10 dB) used for decreasing the sunlight effects. The output voltage from the detector, proportional to the received optical power, is logged using a data acquisition card connected to a computer. Data is collected with an

appropriate sampling rate and stored into the computer in a text file format by Lab View. Collected data is processed in MathCAD.

Figure 5.6 illustrates the first results of the field tests from 30th of June to first of July for 24 hour period. During the test the laser operates at continuous wave mode and the sampling rate at the DAQ card is 1Hz, the temperature and the wind variations are also collected during the observation time period. The maximum power fluctuation seen in this picture can reach to -12 dB. This data has been collected starting at 10:45 am through 09:00 am of next day. At the end of the period the power level at the detector reached the starting level, therefore; a 24-hour cycle in the power fluctuation is observed. It is highly probable to say that the fluctuation in the intensity is due to atmospheric events rather than the system performance degradation.

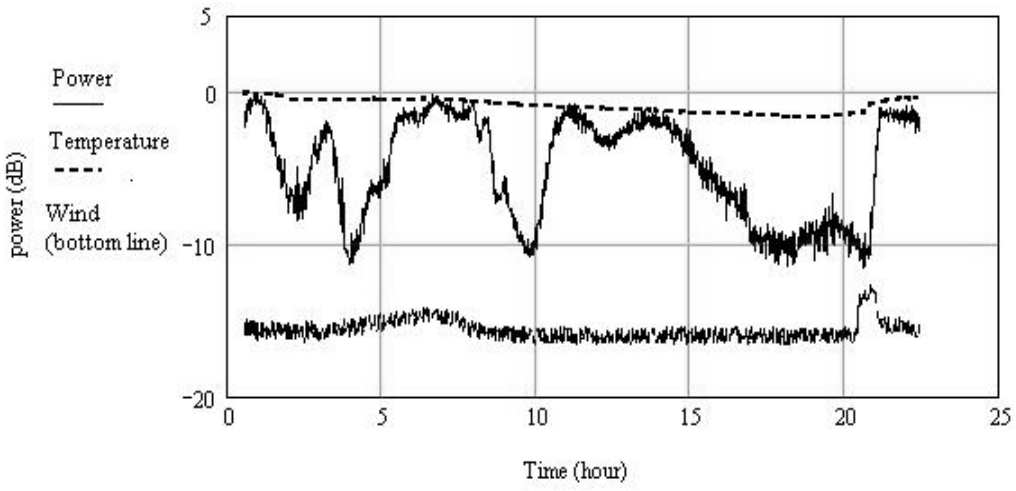

Figure 5.6. 785nm CW laser link observations 29th June-30th July.

The significant correlation between the intensity and weather data can be seen during night time and at the sunrise. The highest wind speed and the temperature variation are observed that related to the dawn, this point is coincident with the sharpest incline of the intensity data. However, after the sunrise there is a deep fluctuation which is not correlated with any weather data.

Figure 5.7 shows the observations carried out for the next 24 hours from 30th of June to the first day of July. Similar to the previous observations the sampling frequency is 1Hz. The second set of data is collected to compare the link behavior in two different days under approximately same atmospheric conditions.

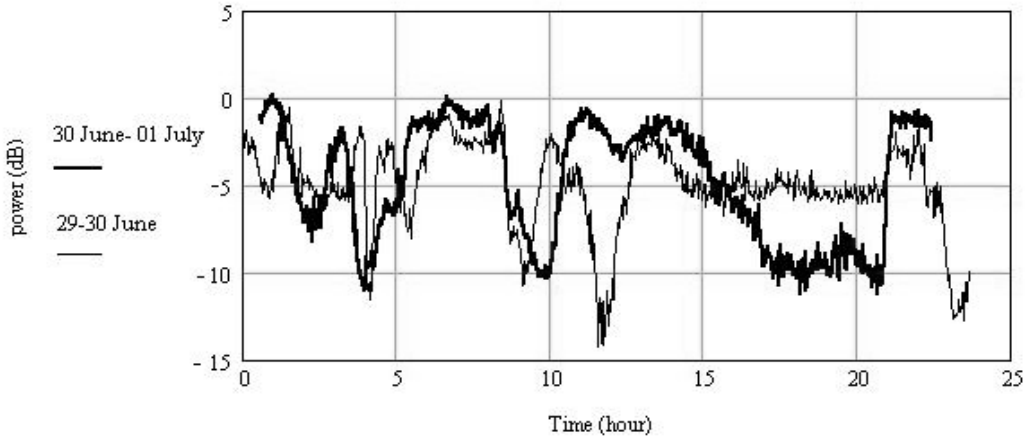

Figure 5.7. 785nm laser link observations at two different days. (29^{th}- 30^{th} June , 30^{th} June-first of July).

Although these two sets of data show similar behavior in terms of the maximum range of the link loss , the maximum and the minimum points are not strictly coincident. And the correlation during the night time and the sunrise is remarkable.

Since the power fluctuation in the morning time is quite high and unpredictable, the detector drift might have been responsible for this problem. In order to clarify this situation the continuous light beam is chopped with a frequency of almost 1 Hz by modulating the laser directly with this frequency. The result is shown in Figure 5.8. Bold line corresponds to the cw light beam while the normal one is for the chopped data (digital). It is hard to tell that the detector is drifting by inspecting this picture, so the chopping is not a solution to this problem. Therefore, these two situations, digital and cw, are not distinguished.

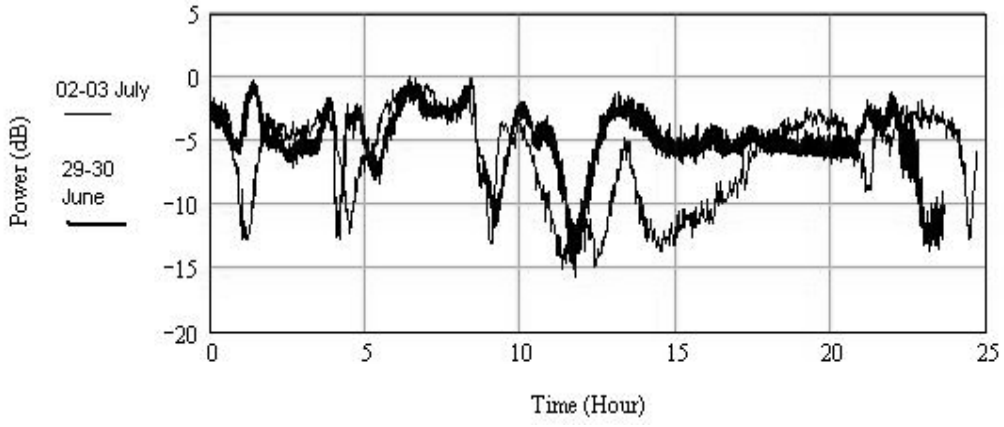

Figure 5.8. 785nm laser link digital (1Hz) data versus CW.

As mentioned in the Chapter 3 and 4 the optical apparatus of the receiver unit can be realized with both bulk optics and Fresnel optics. The beam profile of the Fresnel lenses obtained in our laboratory tests are given in the beginning of this chapter. The beam profiles of the Fresnel lens are found wider and gently declining at the edges. This property is definitely useful for keeping the power fluctuations in a limited band as shown in Figure 5.9. In this picture two different Fresnel lens, having the diameter 5 cm and 12.7 cm, are used and compared with the 5 cm bulk optic lens. The larger Fresnel lens shows a superior power fluctuation with respect to other two options, having that 7 dB power margin. Moreover comparison of the same size Fresnel lens with bulk lens shows that Fresnel lens outperforms the bulk optic power margin, better than 2 dB.

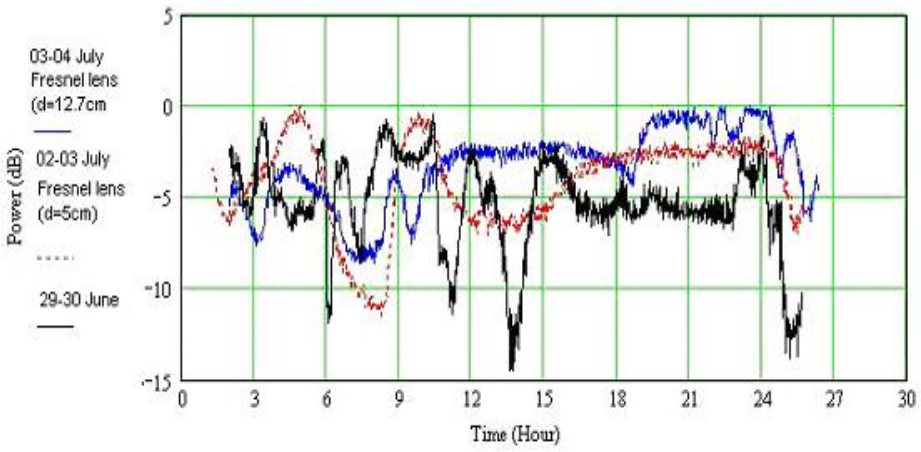

Figure 5.9. Fresnel optic and bulk optic comparison with two Fresnel and a bulk optic lens during 24 hour measurements.

.

By inspecting these results it is possible to say that using Fresnel lens as the optical unit of the receiver system might be a good solution for a non-tracking free space optical link system for better technical and cost performances as claimed in the theoretical model in chapter 4.

5.2.2 1550nm-Laser Link Field Tests

The 1550nm-laser link has been observed from 23rd of July till the 09th of August 2004. Experimental link scheme consists of 5mW FP laser diode. Similar to the 785nm-laser link a bi-convex D=2.54cm lens used for the light collimation and both plano-convex (D=5.08cm) and Fresnel lens (D=12.7cm) used for the light collection. In addition 1550nm line-filter is used to reduce the sunlight effects. All of the observed data is logged to the computer by the data acquisition card.

Figure 5.10 illustrates the results of FSO link where the bulk optic lens as a receiver aperture. During the tests the laser operates like the 785nm-laser at continuous wave mode and the sampling rate is 1Hz at the receiver side. The maximum power fluctuation seen in this picture reaches to -2.5 dB. This data has been collected starting at 16:15 pm through the next 48 hours. At the end of the period the power level at the detector reached the starting level, therefore; a 48-hour cycle in the power fluctuation is observed. It is highly probable to say that the fluctuation is due to the atmospheric events rather than the system degradation.

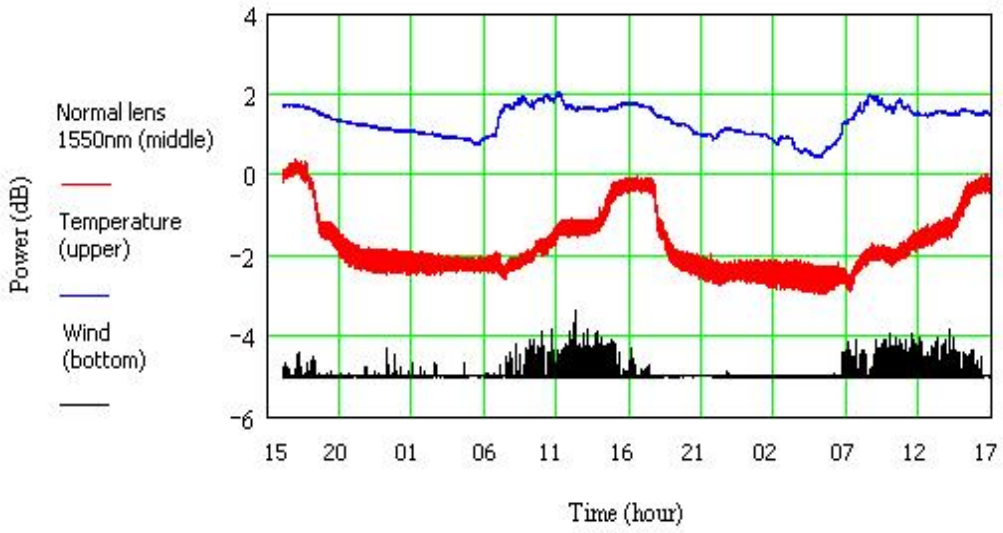

Figure 5.10. 1550nm-laser link observations from 23rd of August to 25th of August.

It is significant that the temperature data and the intensity are showing good correlation during the daytime. The highest temperature variations are observed during the early morning where the sunlight hits the laboratory building. This temperature increase coincident with the inclination of the intensity data. Furthermore it is difficult

to interpret that there is a good correlation between the intensity data and the wind. At certain time intervals a slight correlation can be seen between wind and the intensity.

Figure 5.11 shows the observations carried out for the 48 hours from the 6th of August starting at 16:15pm to the 8th August with the Fresnel lens, which has a diameter of 5cm. Like the previous bulk optic system the laser operates at continuous power and the sampling rate is 1Hz at the receiver side. The maximum fluctuations seen in this picture is 3.2 dB.

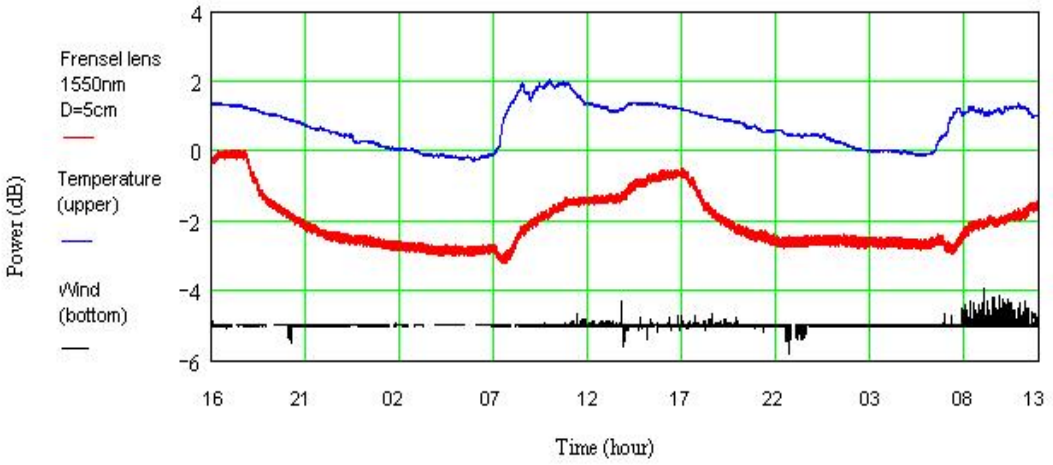

Figure 5.11. 1550nm laser link observation with Fresnel lens (D=5cm) from 6th of August to 8th of August.

Similar to the bulk optic system Fresnel lens link observations show the correlation between the temperature and the intensity level. In addition the wind is partially correlated with the intensity data.

Figure 5.12 illustrates the two Fresnel lenses (D=5cm, D=12.7cm) and the normal lens (D=5cm) observations. In contrast to the 785nm-laser link case both lenses show remarkably reduced power fluctuations which are approximately 3.2 dB. In addition the Fresnel lens shows an extra power loss of approximately 0.7 dB which is due to the focal length difference between bulk optic lenses (Fresnel lens f=25.4cm. Normal lens f=10cm). Moreover both the bulk optic lens and the Fresnel lenses introduce a slight valley during the early morning at 7:30 am in the morning. At that time sunlight enters the laboratory and falls to the transmitter equipment, which might be the possible reason of these fades.

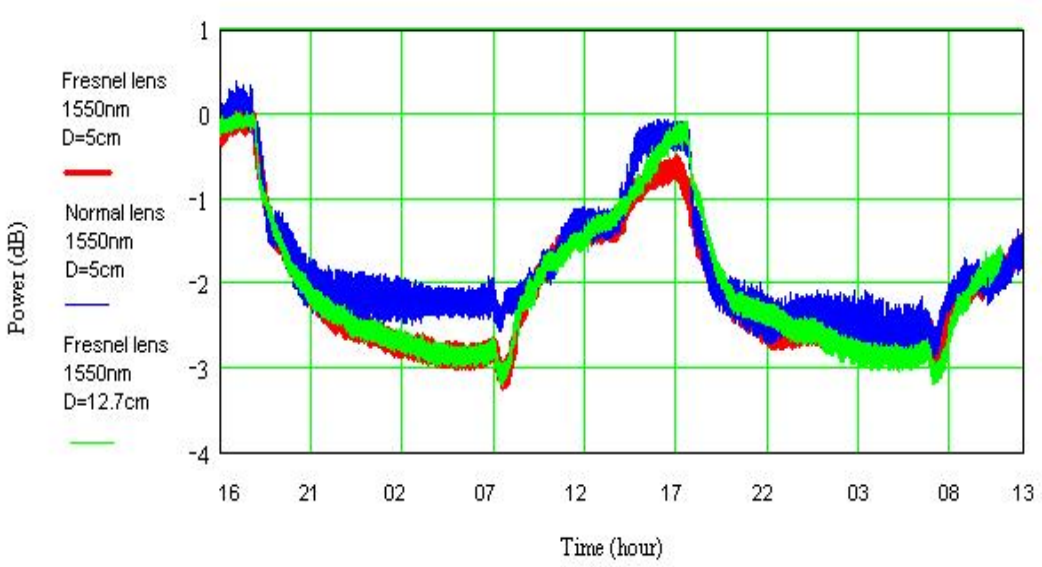

Figure 5.12 1550nm laser-link with Normal lens (D=5cm), Fresnel lens (D=5cm, 12.7cm)

By inspecting these results although there is an extra loss in the power coupling efficiency of Fresnel lenses in contrast to normal lenses, Fresnel lenses might be alternative solution to the bulk optic.

5.2.3 Link Comparison between 785nm and 1550nm

Figure 5.13 shows the observations of both 785nm and 1550nm laser link with bulk optic lens and the 1550nm-laser link with small Fresnel lens as the receiver aperture. The measurements are carried out during the 29th –30th June for the 785nm laser-link and for the 1550nm-laser link days between the second of august till the 8th of August.

As illustrated below 1550nm-laser link has a superior performance in contrast to the 785nm-laser link. The 1550nm link has approximately 8 dB less intensity fluctuation than 785nm link. Moreover the overall system stability is far better than 785nm in 1550nm link. 785nm link introduces several peaks and bottoms during the 24-hour period while there are slowly varying changes in 1550nm link where the peaks and valleys are smaller in size.

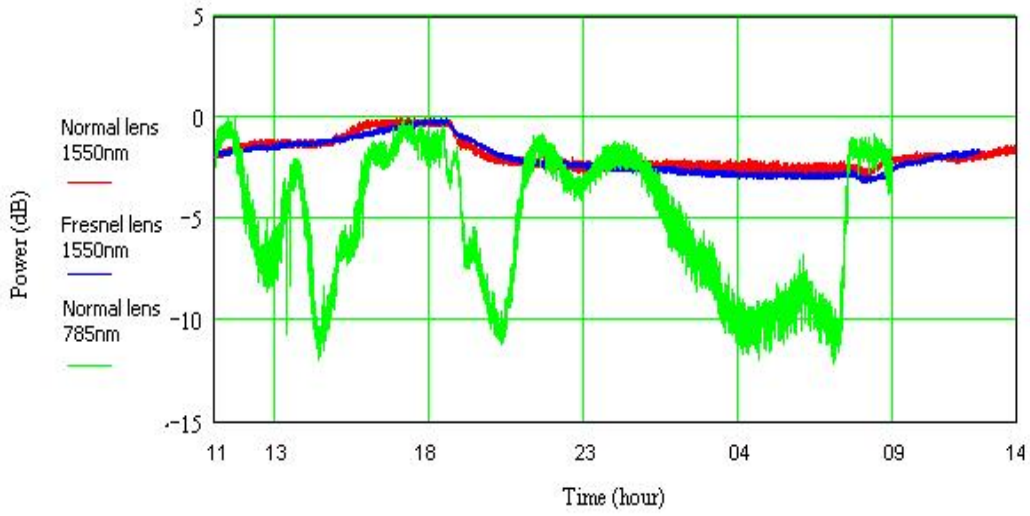

Figure 5.13. 785nm and 1550nm link comparison.

5.3 Conclusion

The proposed FSO transmission link is established for short-distance continuous wave propagation of laser beam between two buildings of the engineering faculty.

As stated in previous chapters large aperture lenses would be a solution to reduce the losses due to the degradation effects. Therefore, the first outcome of the experimental observations has proved that the Fresnel lens with diameter of 12.7cm in the 785nm-laser link gives an extra 7 dB power margin than the bulk optic lens with a diameter of 5cm. Furthermore the small aperture-size (5cm) Fresnel lens is also 3 dB better than bulk optic lens on which 12 dB power margin is measured, which is 15 dB in the bulk optic case. However for the 1550nm-laser link both of the Fresnel lenses (D=5cm and D=12.7cm) perform slightly worse then the bulk optic lens which is about 0.7 dB. When considering the short-range link distance this performance difference could be acceptable due to the increased F.O.V tolerances. For the mid and long range (200m-1km) FSO links, scintillation starts to be considerable which degrades the received power about 2 dB to 5 dB while the observed 0.7 dB loss is considerably low in contrast to 5 dB loss.

Another important result is the better link stability (power fluctuations) of the 1550nm-laser link in contrast to the 785nm-laser link. 785nm-laser link introduces several local minimums and maximums in the transmitted power, which are ranging 5

dB to 12 dB where the 1550nm-laser link is nearly stable over the same operation period. These power fluctuations in 785nm-laser link might be resulted due to the weak robustness of experimental set-up.

Although the temperature variations during the link observations are small in scale, they are highly correlated with the power variations. Furthermore with the different link configurations a slight decline is observed in the received power during the mornings. This situation occurs despite the usage of line filter due to the direct exposure of the sunlight onto the receiver equipment in the morning. In contrast to the temperature, the wind variations are slightly correlated with the power fluctuations and have minor effect on the overall system performance.

One of the other outcomes of this study is to describe required link budget of the link in districts around Izmir. Without considering losses resulting from the transceiver components the overall link budget is 12 dB for 785nm and 4 dB for the 1550nm link in clear air conditions. For the worst scenario (moderate fog) the power margin of the interested link has to be increased 3 dB.

Field-of-view and the displacement tolerances are important issues in non-tracking FSO systems design where these factors can be improved by large aperture sized lenses having small focal length.

REFERENCES

[1] D. Killinger, "*Free Space Optics for Laser Communication Through the Air,"* Optics & Photonics News, pp.36-42, October 2002.

[2] J. Gowar, *Optical Communication*, Prentice Hall, New York 1993.

[3] P. F. Szajowski, J. J. Auborn, G. Nylokak, H. M. Presby an G. E. Tourgee, "*High power optical amplifiers enable 1550nm terrestrial free-space optical data-link operating @ WDM 2.5Gb/s data rates*," Optical Wireless Communication II, proc. SPIE, vol.3850, pp.2-10, 1999.

[4] I. I. Kim, R. Stieger, J. A. Koontz, C. Moursund, M. Barclay, P. Adhikari, J. Schuster, E. Korevaar, "*Wireless optical transmission fast ethernet, FDDI, ATM, and ESCON protocol data using the Terralink laser communication system*," Optical Engineering, Society of Photo-Optical Instrumentation Engineers. Vol.32, No.12, pp. 3143-3155, 1998.

[5] *FSO primer* Media access available via Fsona Optical Wireless Communications http://ww.fsona.com/technology.php?sec=fso_primer.

[6] *FSO solutions* Media access available via Fsona Optical Wireless Communications http://ww.fsona.com/solutions.php.

[7] P.Schoon, "*Free Space Optics in the Enterprise Market*," System Support Solutions Inc., February 2003.

[8] G. Nykolak, G. Raybon, B. Mikkelsen, B. Brown, P.F. Szjowski, J.J. Auborn and H.M. Presby, *" A 160Gb/s Free-Space Transmission Link,"* Optical Wireless Communication III, Proc. SPIE, vol.4214, pp.11-14, 2001.

[9] S. Bloom, E. Korevaar, J. Schuster. H. Willebrand, "*Understanding the performance of free-space optics*," Journal of Optical Networking, Proc. Optical Society of America, vol.2, No:6, pp. 178-200, 2003.

[10] D.Romain, M. Larkin, G. Ghayel, B. Paulson, g. Nykolak, "*Optical wireless propagation, theory vs. Experiment,"* Optical Wireless Communication III, Proc. SPIE, vol.4214, 2001.

[11] I.I. Kim, B. McArthur and E. Korevaar, "*Comparison of laser beam propagation at 785nm and 1550nm in fog an haze for optical wireless communications*," Media access available via http://www.opticalaccess.com/white_papers.

[12] I.I. Kim, M. Mitchell and E. Korevaar," *Measurement of scintillation for free-space laser communication at 785nm and 1550nm*," Optical Wireless Communication II, Proc. SPIE. Vol.3850, pp 49-62, 1999.

[13] E.A. Saleh, M.C. Teich, *Fundamentals of Photonics*, John Wiley & Sons, 1991.

[14] L.H.Schwartz, J.B. Cohen, "*Diffraction from Materials*," Springer-Verlag, Heidelberg, 1987.

[15] *Melles Griot 1997-1998*, Product catalogue.

[16] F. Levander, P.Sakari, " *Design and Analysis of an All-optical Free-space Communication Link*", master thesis, 2002.

[17] *Reflection and Refraction of light (Fresnel formulas)* Media access available via http://physics.nad.ru/Physics/English/rays_txt.htm.

[18] *Edmund Industrial Optics* product catalogue, 2002.

[19] J.M. Wallace and P.V. Hobbs, "*Atmospheric Science: An Introductory survey*," Academic Press, Orlando, 1977.

[20] W.E.K. Middleton, *Vision Through the Atmosphere*, U. of Toronto press, Toronto, 1952.

[21] X. Zhu, J.M. Kahn, "*Free-space optical communication through atmospheric turbulence channels*," IEEE Transactions on Communication, vol.50, No.8, pp. 1293-1300, 2002.

[22] H. Weichel, *Laser Beam Propagation in the Atmosphere*, SPIE, Bellingham WA, 1990.

[23] *Thorlabs product catalogue*, 2004.

[24] E. Hecht, *Optics*, Addison-Wesley, Massachusetts, 1990.

[25] W.B. Wetherell, M.P. Rimmer, " *General analysis of aplanatic Cassegrain, Gregorian and Schwarzhild telescopes*," Applied Optics, vol.11, no.12, 1972.

[26] Fresnel Technologies product catalogue 2004.

[27] J. Alwan, "*Eye Safety and Wireless Optical Networks,*" Airfiber Inc., Media access available http://www.airfiber.com, April 2001.

[28] H. Urey, "*Spot size, depth-of-focus, an diffraction ring intensity formulas for truncated Gaussian beams*," Applied Optics, vol.43, No.3 pp. 620-625, 2004.